JPET Fast Forward. Published on June 18, 2022 as DOI: 10.1124/jpet.122.001119
This article has not been copyedited and formatted. The final version may differ from this version.

Tralesinidase alfa enzyme replacement therapy prevents disease manifestations in a canine model of mucopolysaccharidosis type IIIB

N. Matthew Ellinwood[1,2], Bethann N. Valentine[1], Andrew S. Hess[1], Jackie K. Jens[1], Elizabeth M. Snella[1], Maryam Jamil[1], Shannon J. Hostetter[3], Nicholas D. Jeffery[2], Jodi D. Smith[3], Suzanne T. Millman[4,5], Rebecca L. Parsons[4], Mark T. Butt[6], Sundeep Chandra[7], Martin T. Egeland[8], Ana B. Assis[8], Hemanth R. Nelvagal[8,9], Jonathan D. Cooper[8,9], Igor Nestrasil[10], Bryon A. Mueller[10], Rene Labounek[10], Amy Paulson[10], Heather Prill[7], Xiao Ying Liu[7], Huiyu Zhou[7], Roger Lawrence[7], Brett E. Crawford[7], Anita Grover[7], Ganesh Cherala[7], Andrew C. Melton[7], Anu Cherukuri[7], Brian R. Vuillemenot[7], Jill CM Wait[7], Charles A. O'Neill[7], Jason Pinkstaff[7], Joseph Kovalchin[11], Eric Zanelli[11], Emma McCullagh[7]

Affiliations:

[1] Department of Animal Science, Iowa State University; Ames, IA, USA.

[2] Department of Veterinary Clinical Science, Iowa State University; Ames, IA, USA.

[3] Department of Veterinary Pathology, Iowa State University; Ames, IA, USA.

[4] Department of Veterinary Diagnostics and Production Animal Medicine, Iowa State University; Ames, IA, USA.

[5] Department of Biomedical Science, Iowa State University; Ames, IA, USA.

[6] StageBio; Frederick, MD, USA.

[7] BioMarin Pharmaceutical Inc.; Novato, California, USA.

[8] The Lundquist Institute (formerly Los Angeles Biomedical Research Institute) at Harbor-UCLA Medical Center; Torrance, CA, USA.

[9] Department of Pediatrics; Washington University in St Louis, St Louis, MO, USA.

[10] Department of Pediatrics; University of Minnesota, Minneapolis, MN, USA.

[11] Allievex Corporation, Marblehead, MA, USA.

JPET Fast Forward. Published on June 18, 2022 as DOI: 10.1124/jpet.122.001119
This article has not been copyedited and formatted. The final version may differ from this version.

Running Title Page

Running Title: Efficacy of tralesinidase alfa in a canine model of MPS IIIB

Corresponding Author: N. Matthew Ellinwood
Present address: National MPS Society, Durham North Carolina, USA.
Telephone number: +1 (919) 806-0101
matthew@mpssociety.org

Co-corresponding Author: Emma McCullagh
Present address: Domain Biotechnologies, Inc., Austin, TX, USA.
domainbiotechnologies@gmail.com

Number of text pages: 24
Number of tables: 1
Number of figures: 6
Number of references: 39
Abstract word count: 241
Introduction word count: 748
Discussion word count: 1498

List of nonstandard abbreviations:
aCSF: artificial CSF
ADA: anti-drug antibodies
BBB: blood-brain barrier
BLQ: below the limit of quantitation
CSF: cerebrospinal fluid
C_{max}: maximal concentration
CNS: central nervous system
ERT: enzyme replacement therapy
GAG: glycosaminoglycans

JPET Fast Forward. Published on June 18, 2022 as DOI: 10.1124/jpet.122.001119
This article has not been copyedited and formatted. The final version may differ from this version.

GFAP: glial fibrillary acidic protein

HS: heparan sulfate

HS-NRE: non-reducing ends of HS

IBA-1: ionized calcium binding adaptor molecule 1

ICV: intracerebroventricular, intraventricular

IGF1R: insulin growth factor 1 receptor

IR: insulin receptor

IT-C: intrathecal cervical

IT-L: intrathecal lumbar

K_{uptake}: concentration of enzyme at half-maximal uptake

LAMP1: lysosome-associated membrane protein 1

LLOQ: lower limit of quantitation

LSD: lysosomal storage disease

MPS IIIB: mucopolysaccharidosis type IIIB

MRI: magnetic resonance imaging

NAGLU: N-acetyl-alpha-glucosaminidase

NRE: Non-reducing end

PD: pharmacodynamics

PK: pharmacokinetics

QW: once weekly administration

QOW: once every other week administration

TA: tralesinidase alfa

UA: unaffected littermates

Recommended section assignment: Drug Discovery and Translational Medicine

JPET Fast Forward. Published on June 18, 2022 as DOI: 10.1124/jpet.122.001119
This article has not been copyedited and formatted. The final version may differ from this version.

Abstract

Mucopolysaccharidosis type IIIB (MPS IIIB; Sanfilippo syndrome B; OMIM #252920) is a lethal, pediatric, neuropathic, autosomal recessive, and lysosomal storage disease with no approved therapy. Patients are deficient in the activity of N-acetyl-alpha-glucosaminidase (NAGLU; EC 3.2.150), necessary for normal lysosomal degradation of the glycosaminoglycan heparan sulfate (HS). Tralesinidase alfa (TA), a fusion protein comprised of recombinant human NAGLU and a modified human insulin-like growth factor 2, is in development as an enzyme replacement therapy that is administered via intracerebroventricular (ICV) infusion, thus circumventing the blood brain barrier. Previous studies have confirmed ICV infusion results in widespread distribution of TA throughout the brains of mice and non-human primates. We assessed the long-term tolerability, pharmacology, and clinical efficacy of TA in a canine model of MPS IIIB over a 20-month study. Long-term administration of TA was well-tolerated as compared to administration of vehicle. TA was widely distributed across brain regions, which was confirmed in a follow-up 8-week pharmacokinetic/pharmacodynamic study. MPS IIIB dogs treated for up to 20 months had near-normal levels of HS and HS-NRE in CSF and central nervous system (CNS) tissues. TA-treated MPS IIIB dogs performed better on cognitive tests, had improved CNS pathology and decreased cerebellar volume loss relative to vehicle-treated MPS IIIB dogs. These findings demonstrate the ability of TA to prevent or limit the biochemical, pathological, and cognitive manifestations of canine MPS IIIB disease, thus providing support of its potential long-term tolerability and efficacy in MPS IIIB subjects.

JPET Fast Forward. Published on June 18, 2022 as DOI: 10.1124/jpet.122.001119
This article has not been copyedited and formatted. The final version may differ from this version.

Significance Statement

This work illustrates the efficacy and tolerability of tralesinidase alfa as a potential therapeutic for MPS IIIB patients by documenting that direct CNS administration to MPS IIIB dogs prevents accumulation of disease-associated GAGs in lysosomes, hepatomegaly, cerebellar atrophy, and cognitive decline.

JPET Fast Forward. Published on June 18, 2022 as DOI: 10.1124/jpet.122.001119
This article has not been copyedited and formatted. The final version may differ from this version.

Introduction

Mucopolysaccharidosis type IIIB (MPS IIIB; Sanfilippo syndrome B), is a devastating and currently untreatable ultrarare neuropathic lysosomal storage disease (LSD) caused by autosomal recessive inherited loss of activity of N-acetyl-alpha-glucosaminidase (NAGLU; EC 3.2.150), one of the four enzymes associated with Sanfilippo syndrome. Deficient NAGLU activity results in lysosomal accumulation of its substrate, the glycosaminoglycan (GAG) heparan sulfate (HS) (Neufeld and Muenzer 2019). Estimated incidence of all four MPS III types ranges from 0.28 to 4.1 per 100,000, with a global birth prevalence of MPS IIIB estimated at 0.21 per 100,000 (Valstar et al. 2008; Kong et al. 2021). Children appear normal at birth, but between the ages of 1 to 4, they experience developmental delay, seen prominently as speech more than motor delay, and global loss of early milestones, progressing to a cognitive decline (Nidiffer and Kelly 1983; Shapiro et al. 2016). As disease progresses, children enter a hyperkinetic phase with severe hyperactivity, sleep-wake disturbance, loss of impulse control, gastrointestinal dysfunction, and continued intellectual decline. Symptoms wane with the onset of a quiescent phase associated with progressive neurodegeneration and dementia, leading to death, typically in the second to third decade of life. Disease course is predictable, but with a variable timeline (Valstar et al. 2011). Clinical decline seen on cranial MRI includes global neuronal loss, ex vacuo dilatation of the lateral ventricles, cortical brain atrophy and white matter abnormalities (Zafeiriou et al. 2001).

Disease causing variants in the *NAGLU* gene result in deficient NAGLU activity and primary pathological lysosomal accumulation of undegraded HS with N-acetylglucosamine terminating non-reducing ends (HS-NRE). Based on human and animal model studies of Sanfilippo syndrome, prominent lysosomal accumulation of HS and secondary metabolic products are seen in cells of the central nervous system (CNS), visceral organs (often associated with hepatosplenomegaly), and the reticuloendothelial system (Jones et al. 1997; Li et al. 1999; Ellinwood et al. 2011).

Conventional intravenous enzyme replacement therapy (ERT) is not a viable treatment strategy for MPS IIIB. Attempts to overexpress NAGLU lead to low levels of mannose-6-phosphorylation (M6P), limiting enzyme uptake by cells (Zhao and Neufeld 2000; Weber, Hopwood, and Yogalingam 2001). However, preliminary studies with recombinant human

JPET Fast Forward. Published on June 18, 2022 as DOI: 10.1124/jpet.122.001119
This article has not been copyedited and formatted. The final version may differ from this version.

NAGLU (rhNAGLU) cis-tagged with an insulin like growth factor 2 (IGF2) ligand domain documented robust M6P-mediated uptake and pharmacologic activity in MPS IIIB mice (Kan, Troitskaya, et al. 2014; Kan, Aoyagi-Scharber, et al. 2014).

Tralesinidase alfa (TA), a fusion protein comprised of rhNAGLU and a modified human insulin-like growth factor 2 (IGF2), is being developed as an ERT for the treatment of MPS IIIB. To circumvent the blood-brain-barrier (BBB), a necessity to resolve the brain pathology central to MPS IIIB, TA is administered directly into the CSF by intracerebroventricular (ICV) infusion via the lateral ventricle of the brain. ICV administration of TA in a murine MPS IIIB model led to widespread brain distribution, reduced neuropathology, decreased lysosomal burden, and significant reduction of HS in brain tissues as assessed by both a conventional HS assay as well as with an assay measuring the MPS IIIB disease specific non-reducing end form of HS (HS-NRE) (Aoyagi-Scharber et al. 2017). Follow up studies in MPS IIIB mice and normal non-human primates further documented the efficacy and distribution of TA within the brain (Grover et al. 2020).

Larger animal model of the mucopolysaccharidoses have been critical to the advancement of therapies (Haskins et al. 2002) and are well-suited to preclinical confirmation of the safety, efficacy, and pharmacologic activity of potential therapeutics. The canine MPS IIIB model is well characterized at the clinical, genetic, biochemical, and neuropathologic level (Ellinwood et al. 2003; Egeland et al. 2020; Raj, Ellinwood, and Giger 2020; Harm et al. 2021), and has been used in preclinical therapeutic evaluations (Ellinwood et al. 2011). MPS IIIB dogs are deficient in NAGLU activity and show accumulation of HS in the CSF, CNS tissue, peripheral tissue, urine, and plasma, detectable as early as one month of age (Ellinwood et al. 2003; Egeland et al. 2020). Animals develop normally, with clinical signs appearing around 2 years of age, including hepatomegaly and progressive cerebellar disease with tremors, dysmetria, and ataxia, and require humane euthanasia between 3 to 5 years of age (Ellinwood et al. 2003). End-stage CNS histopathology includes severe cerebellar atrophy, Purkinje cell loss, neuroaxonal dystrophy, microglial activation and vacuolation, gliosis, and granular storage vacuoles in neurons. The studies described herein evaluate the therapeutic efficacy of TA administration in preventing or limiting these disease manifestations in this canine MPS IIIB model, and support TA therapy for MPS IIIB.

JPET Fast Forward. Published on June 18, 2022 as DOI: 10.1124/jpet.122.001119
This article has not been copyedited and formatted. The final version may differ from this version.

JPET Fast Forward. Published on June 18, 2022 as DOI: 10.1124/jpet.122.001119
This article has not been copyedited and formatted. The final version may differ from this version.

Materials and Methods

Animal studies. Animal production, maintenance, transit, transfer, and experimental studies were carried out in accordance with the Guide for the Care and Use of Laboratory Animals and under protocols approved by the authorized Institutional Animal Care and Use Committees.

The Materials and Methods presented here refer to the long-term safety and efficacy study conducted in MPS IIIB dogs. Materials and Methods for the supplemental 8-week PK/PD study are described in the Supplementary Information.

TA and vehicle control articles. TA was provided by BioMarin Pharmaceutical Inc. TA was formulated in artificial CSF (aCSF; 148 mM NaCl, 3mM KCl, 0.8 mM MgCl2•6H2O, 1.4 mM CaCl2•2H2O, 0.7 mM Na2HPO4, 0.3 mM NaH2PO4, pH 7.0) at a concentration of ~ 5 mg/ml (12 mg dose level) or ~20 mg/ml (48 mg dose level).

Animals. Dogs in the study were housed in an Iowa State University (ISU) Lab Animal Resource managed facility and were managed according to guidelines of the USDA and the NIH. Dogs were fed at libitum with Teklad maintenance or growth diet. Dogs were given filtered municipal water *ad limitum*. The MPS IIIB dogs and unaffected littermate control dogs were produced from breedings of MPS IIIB carrier females to MPS IIIB or carrier males within an outbred colony maintained at ISU. Animals were diagnosed shortly after birth by PCR screening to confirm their NAGLU genotype (Raj, Ellinwood, and Giger 2020), and were tattooed with an identification number at approximately 8 weeks of age.

Surgery. Dogs of approximately 4 months of age were implanted with catheters to a lateral cerebral ventricle for dose administration and to the lumbar spine (IT-L) for serial CSF collection. MRI was performed as described to implant the ICV catheter appropriately (Vuillemenot et al. 2014). Surgical and post-surgical recovery and monitoring procedures were designed and approved to ensure full analgesia and pain management.

Study design. The study design is outlined in Table 1 and Supplementary Figure 1A. Dogs were enrolled as puppies as the required genotypes became available. Dogs were administered a low dose of TA (0.58 mg/kg; Groups 2 & 3) or vehicle (Phosphate buffer pH 7.0; Groups 1) via IV infusion for 10 administrations between 1 and 13 weeks of age for desensitization purposes (Dierenfeld et al. 2010). Beginning at approximately 4.5 months of age, dogs began receiving

JPET Fast Forward. Published on June 18, 2022 as DOI: 10.1124/jpet.122.001119
This article has not been copyedited and formatted. The final version may differ from this version.

ICV administration of ~2.4 ml vehicle (aCSF) or 12 or 48 mg TA every other week (QOW) via a slow infusion over 4 hours using a syringe pump (0.6 ml/hr). When ICV catheters were no longer patent, doses were infused via the IT-L catheter or via bolus isovolumetric IT-C injection after removing ~3 ml of CSF via the IT-C puncture. To address the potential for complications due to catheter patency and port contamination, all administrations were switched to isovolumetric IT-C infusions between doses 7 and 23. For clarity, administration of vehicle and TA will be referred to as direct CNS administration throughout the text.

Additionally, unaffected littermates (homozygous normal dogs or heterozygous carriers) were enrolled in the study, implanted with ICV and IT-L catheters and were used as controls in the experiments described herein. Due to logistical and technical difficulties, not all dogs could be analyzed in every endpoint. The number of dogs used in each analysis will be provided when applicable.

Clinical signs and clinical pathology. Dogs were observed for clinical signs, morbidity, and mortality at least once daily post-surgery and throughout the study periods. Blood glucose and fructosamine levels were measured pre study, study weeks 13, 27, 41, 55, 69, and at the end of study (study week 83, Supplementary Figure 1A).

PK and antibody analysis. Pharmacokinetic samples were obtained from CSF of MPS IIIB dogs administered 48 mg TA from the lumbar before the ICV infusion start (pre-dose), halfway into the infusion (at 2 hours), immediately after the end of the infusion (~2 minutes post dose), and at 0.5, 2-, 6-, 10-, 24-, 48-, 72-, 96-, 120- and 168-hours post-dose at study weeks 37, 40, 55, 69, and 83 (end of study, Supplementary Figure 1A). Only 2 of the MPS IIIB dogs in Group 3 (Table 1) had patent catheters at any of the doses to sample CSF for PK analysis. CSF for PK analysis was transferred into vials containing 1% Tween-20, for a final concentration of 0.05% Tween-20. TA levels were measured as described (Grover et al. 2020). CSF samples for total anti-drug antibody (ADA) analysis were collected prior to dose administration when possible (patent IT-L catheters). Total anti-TA antibody levels in CSF were analyzed using an electrochemiluminescent immunoassay technology platform (ICON Laboratory Services, Whitesboro, NY).

CNS TA biodistribution. Within 72 hours following the final dose, dogs on study were euthanized and 4-mm round biopsy punches were collected from surface (<3 mm from closest

JPET Fast Forward. Published on June 18, 2022 as DOI: 10.1124/jpet.122.001119
This article has not been copyedited and formatted. The final version may differ from this version.

CSF flow) and deep (>3 mm from the closest CSF flow) regions of the brain (frontal cortex, striatum, thalamus, midbrain, occipital cortex, cerebellum, and medulla). Additionally, 1 cm sections of the cervical, thoracic, and lumbar spinal cord were collected. Samples were immediately frozen at -80 C and TA levels were measured as described (Grover et al. 2020).

Histopathology. Histopathological safety assessment of the CNS and peripheral tissues was conducted. Serial coronal sections from throughout the brain were collected and analyzed for markers of neuronal changes. In addition to brain sections, peripheral tissues including liver and kidney were embedded in paraffin and stained with H&E. As part of the safety assessment, all tissues were examined and scored by a board-certified veterinary pathologist (StageBio, Frederick MD) using the validated Custom Workbook for Pathology Data system (version 2.1).

PD marker analysis. Tissue punches from brain regions and spinal cord from dogs on study were collected at the time of necropsy (within 72 hours of final dose). CNS tissue samples were pooled for each of the dogs to reduce the potential for punch-to-punch variability. CSF samples were collected just prior to the final dose. Total HS (referred to as HS) and MPS IIIB-specific HS-NRE levels were quantified in CSF and homogenized CNS tissue using the Sensi-Pro assay, which is an adaptation of GRIL-LC/MS and has been described previously (Lawrence et al. 2012; Lawrence et al. 2014; Aoyagi-Scharber et al. 2017). Two labs carried out the CSF and CNS tissue assays using different but equivalent methods of HS quantitation (BioMarin Pharmaceutical Inc.) The two most abundant internal disaccharides of HS were quantified in CSF and the same two disaccharides plus four lower abundance disaccharides were measured in CNS tissue. For correlation analysis only the two most abundant internal disaccharides were used for both CSF and CNS tissue. HS-NRE was quantified by the amount of glucosamine-N-acetate α1,4 iduronate-2-sulfate α1,4 glucosamine 2-N- sulfate trisaccharide (A0I2S0) in both CSF and CNS tissue assays. HS and HS-NRE are expressed as μg/ml (CSF) or pmol/mg tissue weight (CNS tissue). The LLOQ for the CSF assay was 0.035 and 0.01 μg/ml for HS and HS-NRE, respectively.

MRI. MRI evaluations were conducted on MPS IIIB and unaffected littermate dogs from Table 1 over 6 sessions starting at approximately 8 months of age (Session 1) and ending at 24 months of age (Session 6, Supplementary Figure 1A). The intervening sessions occurred approximately every 3 months. MRI acquisition (3D high-resolution T1-weighted magnetization-prepared rapid

JPET Fast Forward. Published on June 18, 2022 as DOI: 10.1124/jpet.122.001119
This article has not been copyedited and formatted. The final version may differ from this version.

gradient-echo, MPRAGE, pulse sequence) was performed on a 3 Tesla Siemens Prisma system with Tx/Rx 15-channel knee coil at the University of Minnesota-Twin Cities. Logistical constraints prevented collection of data from some animals and limited data collection on other animals. Volumes assessed included total brain, cerebral white matter, cerebral gray matter, ventricles, brainstem, cerebellar white matter, and cerebellar gray matter volumes. Total cerebellum and brainstem were manually outlined following the canine atlas (Singer 1962). After brain extraction using FSL brain extraction tool (BET) (Jenkinson et al. 2012) and manual correction of BET inaccuracies, cerebral and cerebellar subvolumes were derived using FSL FAST (FMRIB's Automated Segmentation Tool) (Zhang, Brady, and Smith 2001). All MRI data were collected and analyzed by individuals blinded to the genotype and treatment status of the dogs.

Neuropathology. MPS IIB-associated neuropathology markers were evaluated in brain tissue samples taken at time of necropsy from dogs in Table 1. LAMP1 (a surrogate marker for storage material accumulation; Abcam AB24170, 1:500), IBA-1 (a marker that reflects microglial activation state; Abcam AB5076, 1:1000), and GFAP (a marker of astrocytosis; Dako, now Agilent, Z0334, 1:2000) immunostaining was analyzed in brain regions as described (Egeland et al. 2020).

Cognition. A reversal learning T-maze was adapted from previously published protocols (Laughlin and Mendl 2000; Wang et al. 2007; Sanders et al. 2011). Five total sessions were conducted over the study period to assess learning, and working, short-term, and long-term memory. The first session (Session 1) occurred at approximately 14.2 months of age and the last session (Session 5) occurred at approximately 23.5 months of age, with the intervening sessions occurring approximately every 10 weeks (Supplementary Figure 1A). The acquisition and processing of all data from these evaluations was done by individuals blinded to the genotype and treatment status of the animals. Due to technical issues, not all sessions were conducted on all animals over the course of the study. However, the available data allows for the assessment of disease progression and treatment effects.

Briefly, the T-maze required dogs to enter the maze and then make a choice of one of two arms, one of which was baited with accessible bait (baited) and one of which contained inaccessible bait (sham). Prior to the test sessions, dogs were individually acclimatized to the set-up and trained in the maze. The test sessions consisted of 5 phases. The preferred arm of the maze of

JPET Fast Forward. Published on June 18, 2022 as DOI: 10.1124/jpet.122.001119
This article has not been copyedited and formatted. The final version may differ from this version.

each dog was determined and the dogs were trained to associate the baited preferred arm with a "correct" visual symbol and the sham non-preferred arm with an "incorrect" visual symbol. Dogs were then run through 3 reversal learning phases in which the bait and "correct" visual symbol were switched between the non-preferred arm and the preferred arm. Key outcomes for the T-maze include measures associated with the dogs' performance associated with reaching criteria in the three reversal learning phases as previously described (Sanders et al. 2011). Specifically, the number of errors that the dogs made after the first correct choice during the reversal learning tasks was used to evaluate the dogs' cognitive abilities and understand the effects of MPS IIIB disease status and TA administration on learning and memory.

Statistical analyses. Statistical analyses were conducted using GraphPad Prism version 9.3.1 Statistical tests used are described in the text and in the figure legends.

RESULTS

Safety and PK

Direct CNS administration to MPS IIIB dogs or unaffected littermates of up to 48 mg of TA biweekly for up to 20 months was well-tolerated and did not generate clinical signs of CNS or systemic toxicity. Hypoglycemia could be a potential clinical consequence of the interaction of the IGF2 tag of TA with either the IGF1R or the insulin receptor (IR) in blood. However, no abnormal blood glucose levels were observed during the course of the study (Supplementary Figure 2A). Additionally, fructosamine levels, which reflect glucose changes over the previous 2 to 3 weeks, were similarly unaffected by TA treatment (Supplementary Figure 2B).

Similar to previously published observations in nonhuman primates (Grover et al. 2020), TA distributed widely to superficial and deep brain regions relative to the ventricle. In dogs administered 48 mg TA, the CSF C_{max} ranged from 944 to 2030 μg/ml (n = 2 dogs over 5 doses). ADA were detected in the CSF of 7/8 dogs in Groups 2 and 3 despite the desensitization protocol used (Supplementary Table 1). No dogs in Group 1 had measurable ADA in the CSF.

A follow-up 8-week PK/PD study was conducted to investigate the PK of TA (Supplementary Information, Supplementary Figure 1B, Supplementary Table 2). CSF exposures of TA were consistent throughout the 8-week treatment duration (Supplementary Table 3). After the first

JPET Fast Forward. Published on June 18, 2022 as DOI: 10.1124/jpet.122.001119
This article has not been copyedited and formatted. The final version may differ from this version.

dose, plasma exposures of TA were 3-5 log orders lower in magnitude compared to CSF exposures. None of the dogs in the PK/PD study had detectable ADAs prior to dose 1 and all dogs developed ADA responses in serum and/or CSF by the end of the study (Supplementary Table 4). ADA levels in the CSF were lower over the 8-week study as compared to ADA levels in serum. While the presence of ADA appears to have minimal impact on the PK of TA at earlier doses, a trend towards reduced exposures and half-life were noted in CSF and plasma (Supplementary Figure 3, Supplementary Table 3). Despite the presence of ADA, pharmacologic and pharmacodynamic effects of TA were observed over the course of both studies suggesting that ADA were not neutralizing and/or that the dose level and frequency was sufficient to dose over any neutralizing effects.

HS accumulation in the CNS

Direct CNS administration of TA every two weeks (long-term efficacy study) to MPS IIIB dogs resulted in a statistically significant, dose-dependent reduction of HS and HS-NRE levels in both CSF and CNS tissue compared with MPS IIIB dogs treated with vehicle (Figure 1). HS and HS-NRE levels in CSF and CNS tissue of MPS IIIB dogs treated every other week with 48 mg TA were reduced to near-normal levels.

Correlation analyses of HS and HS-NRE levels in time-matched CSF and CNS tissue samples were conducted to determine whether CSF levels of these PD markers predicted CNS tissue levels (Figure 2). Since similar reductions in HS levels in the CSF and CNS tissue were observed in MPS IIIB dogs from both the long-term efficacy study and the 8-week PK/PD study, data from the two studies were combined to increase statistical power. HS-NRE levels in the CSF and CNS tissue from dogs in the 8-week PK/PD study were below the limit of quantitation (BLQ) so only HS-NRE data from dogs in the long-term efficacy study were included in the correlation analysis. Strong correlations were observed between CSF and CNS tissue for HS ($r = 0.89$) and HS-NRE ($r = 0.85$), indicating that levels of these biomarkers in CSF predict CNS tissue levels.

Neuropathology

Based on an understanding of canine MPS IIIB neuropathology, we characterized the effects of TA administration within the more severely affected regions of the brain, including the cerebellum. TA treatment via direct CNS administration for up to 20 months (long-term efficacy study) led to significant dose-dependent reduction in LAMP1 immunoreactivity in various brain

JPET Fast Forward. Published on June 18, 2022 as DOI: 10.1124/jpet.122.001119
This article has not been copyedited and formatted. The final version may differ from this version.

regions of treated MPS IIIB versus untreated MPS IIIB dogs (Figure 3A, P = 0.005, 2-way ANOVA; representative images in Supplementary Figure 4). The LAMP1 immunostaining intensity was significantly lower in the somatosensory cortex (P = 0.0003) and cerebellar granular layer (P = 0.002) of MPS IIIB dogs treated with TA 48 mg vs. vehicle (Figure 3A). Decreased LAMP1 immunostaining after TA treatment correlated in a linear fashion (r=0.76 and r=0.83 for cerebellum and cortex, respectively) with CSF HS-NRE concentrations (Figure 3B), and the lowest levels of LAMP1 immunostaining were seen in animals with CSF HS-NRE levels at the lowest level of quantification (LLOQ) following TA treatment at the 48 mg dose (Figure 3B).

Reductions of the disease-associated neuroimmune response were observed in MPS IIIB dogs treated with TA. Marked reductions in microgliosis (Figure 3C) and astrocytosis (Figure 3D) were noted in regions of the cerebellum. Immunostaining of IBA-1, a marker of microglial activation, was reduced in a dose-dependent manner in treated MPS IIIB dogs (representative images in Supplementary Figure 4). Although the effects were not statistically significant by one-way ANOVA, there was a TA dose-dependent effect on microglial activation, which was largely confined to the cerebellar white matter. Similarly, astrocytosis in the cerebellum, as assessed by quantitative GFAP immunostaining, showed a dose-dependent decrease in the molecular layer of the cerebellum (Bergmann glia) and was reduced in the Purkinje layer of the cerebellum in MPS IIIB dogs treated with TA (P = 0.03, one-way ANOVA; representative images in Supplementary Figure 4).

These results support a therapeutic and dose-dependent pharmacological effect of direct CNS administration of TA upon a range of neuropathological changes associated with MPS IIIB in the forebrain and the cerebellum. Consistent with these findings, routine histopathology conducted on dogs from Group 1 in Table 1 as part of a safety assessment noted disease-related neuronal vacuolation in the brain and spinal cord, and these changes were notably less pronounced in TA-treated MPS IIIB dogs.

Somatic MPS IIIB pathology including hepatomegaly

Histopathology analysis on dogs from the long-term efficacy study revealed MPS IIIB-related morphological changes in several peripheral tissues including vacuolation in hepatocytes. Indeed, similar to the human form of the disease, dogs with MPS IIIB were found to have

JPET Fast Forward. Published on June 18, 2022 as DOI: 10.1124/jpet.122.001119
This article has not been copyedited and formatted. The final version may differ from this version.

enlarged livers compared to unaffected dogs (Figure 4A). Treatment with TA directly into the CNS resulted in a dose-dependent decrease in liver volume in dogs in the long-term efficacy study (Figure 4A). The MPS IIIB dogs treated with 48 mg TA maintained the liver size observed in unaffected littermates. Furthermore, there was a highly significant, linear correlation ($r = 0.95$ $P < 0.0001$) between CSF HS-NRE concentration and liver weight for treated and untreated MPS IIIB dogs (Figure 4B).

Cerebellar atrophy

Brain MRI evaluations were performed on MPS IIIB dogs from the long-term efficacy study and unaffected littermates approximately every 7 weeks starting at 8 months of age (Session 1) and ending at 2 years of age (Session 6). Image acquisition and analyses were conducted to characterize volumetric changes due to disease progression and the effects of TA treatment. No changes over time were observed in cerebral or brain stem volumes in MPS IIIB dogs compared to unaffected littermates. Conversely, an increase in cerebellar CSF volume was observed over time in vehicle-treated MPS IIIB dogs compared to unaffected littermates, reflecting a loss of cerebellar tissue. TA treatment preserved cerebellar tissue volume in a dose-dependent and a statistically significant manner as measured by a decrease in cerebellar CSF volume in the MPS IIIB dogs treated with 48 mg TA relative to unaffected littermates (Figure 5A, $P = 0.0127$, Dunnett's multiple comparison test). Cerebellar CSF volumes of dogs measured in the final MRI session, conducted when the dogs were approximately 2 years of age, showed a linear correlation (simple linear regression, $r = 0.80$, $P = 0.0098$) with HS-NRE levels in the CSF at necropsy (Figure 5B).

Cognition

Potential treatment effects of TA on cognition, specifically learning and memory, were evaluated in MPS IIIB dogs in the long-term efficacy study and unaffected littermates by using a reversal learning T-maze to assess learning, working, short-term and long-term memory over 5 sessions throughout the 20-month study period beginning when the dogs were approximately 14 months of age. Key outcomes for the T-maze include performance measures associated with reaching criteria in the three reversal learning phases. Specifically, the number of errors that the dogs made after the first correct choice during the reversal learning tasks was used to evaluate the

JPET Fast Forward. Published on June 18, 2022 as DOI: 10.1124/jpet.122.001119
This article has not been copyedited and formatted. The final version may differ from this version.

dogs' cognitive abilities and understand the effects of MPS IIIB disease and TA treatment on learning and memory.

As expected, and as an internal validation of the method, unaffected littermate dogs make fewer mistakes in the T-maze over the 5 sessions, indicative of learning over time (Figure 6A,B). In contrast, MPS IIIB dogs receiving vehicle committed increasing numbers of errors over the 5 sessions, indicating degradation of learning and memory abilities (Figure 6A, B). The MPS IIIB dogs treated with 48 mg TA showed a trend toward improved performance over those treated with 12 mg (Figure 6A); learning ability in the 48 mg dose group was similar to unaffected dogs and better than vehicle-treated MPS IIIB dogs. To increase the statistical power, data from the two TA treatment groups were combined and a significant improvement in performance indicative of learning was observed in unaffected and TA-treated MPS IIIB dogs over the 5 sessions (Figure 6B; $P = 0.03$ for unaffected dogs and $P = 0.029$ for TA-treated dogs when comparing session 1 to session 5 for the same animals, adjusted T test).

DISCUSSION

These studies examine the safety, pharmacology, pharmacodynamics, pharmacokinetics and clinical efficacy endpoints of direct CNS administration of TA in a canine model of MPS IIIB. Given the primarily neurological manifestations of MPS IIIB disease, TA is administered directly into the CNS to circumvent the BBB and allow for wide distribution in the brain. Indeed, the C_{max} of TA measured in the CNS tissue of dogs was well above the K_{uptake} measured in MPS IIIB human fibroblasts (Yogalingam et al. 2019) resulting in widespread distribution throughout the brain and periphery. Consistent with results from other CNS administered ERTs such as cerliponase alfa and arylsulfatase A (Vuillemenot et al. 2014; Troy et al. 2020), TA was detected in the periphery suggesting that there is exchange between the CNS and peripheral compartments perhaps via the glymphatic drainage. Plasma exposures were significantly lower than in the CSF and were generally below the limit of quantification after the initial dose. While these PK characteristics are in line with other ICV administered drugs, it is not possible to rule out potential interference effects of ADA on the quantification of TA. The PK immunoassay relies on antibody detection reagents with specificity for NAGLU and the IGF2-tag. Epitope-specificity of total ADA was not characterized and so it is unknown whether the drug-binding epitopes resulted in interference and lowering of signal detected in the PK assays.

JPET Fast Forward. Published on June 18, 2022 as DOI: 10.1124/jpet.122.001119
This article has not been copyedited and formatted. The final version may differ from this version.

The overt clinical stage of canine MPS IIIB disease is associated with severe movement abnormalities (Ellinwood et al. 2003) and occurs at approximately 2 years of age, which was just the age of the dogs at the time of necropsy in the long-term safety and efficacy study. As such, alternative and sensitive quantitative techniques were used to capture early manifestations of the disease and potential pharmacologic effects of TA.

Total HS and the HS-NRE can be measured quantitatively and have been shown to accumulate in several tissues in MPS IIIB dogs at as early as 1 month of age (Egeland et al. 2020; Ellinwood et al. 2003). Direct CNS administration of TA resulted in a significant and sustained reduction to near-normal levels of these markers in the CSF and CNS tissue in both studies presented here suggesting widespread distribution and uptake despite the appearance of anti-drug antibodies in the CSF. TA is active in the lysosomal compartment and the beneficial reduction of disease-specific markers suggests receptor-mediated uptake and internalization of the enzyme into target lysosomes were not inhibited by ADA either in the CSF or serum. The results from these studies suggest that antibodies generated to TA were not neutralizing and/or that the dose level and frequency were sufficient to overcome any neutralizing effects. Despite the presence of ADA, and low TA levels detected in plasma, hepatomegaly was prevented in a dose-dependent fashion after 20 months of treatment providing further evidence that serum ADA had no apparent neutralizing effect. However, neutralizing antibodies were not specifically measured in these studies. Every other week dosing in the long-term efficacy study and weekly dosing in the PK/PD study similarly reduced the pharmacodynamic markers to near-normal levels suggesting that either dose frequency could be possible to attain clinical efficacy.

Effects of TA treatment on HS and HS-NRE levels in CSF and CNS tissue are highly correlated. These findings validate and support the use of HS and HS-NRE levels in the CSF as surrogates for treatment effects on the levels in CNS tissue since brain tissue cannot be biopsied in the clinic. Although the HS assay used in the studies presented here detects the total HS levels present, the HS-NRE assay specifically detects a moiety on HS that is a substrate for lysosomal NAGLU and, therefore, is only measurable in MPS IIIB dogs where NAGLU activity is abrogated. The intralysosomal accumulated HS in MPS IIIB disease, which contains the MPS IIIB-specific non-reducing ends, is thought to be the basis of disease-related pathophysiology in the CNS and visceral organs. Although immunostaining for HS is possible (Jones et al. 1997), the post-mortem tissue processing for histological analysis inevitably results in loss of HS due to

JPET Fast Forward. Published on June 18, 2022 as DOI: 10.1124/jpet.122.001119
This article has not been copyedited and formatted. The final version may differ from this version.

its highly soluble nature. Thus, quantification of HS by immunostaining would be inaccurate since the technique is compromised by the artifacts associated with HS solubility. The methods of direct quantitative evaluation of HS-NRE by immunostaining are not compatible with histology. For these reasons, and as previously described (Egeland et al. 2020), LAMP1 was used to evaluate the lysosomal compartment as a proxy for intralysosomal accumulation of HS. Therefore, HS-NRE levels, combined with the LAMP1 level on immunostaining (Figure 3B), provide a direct and specific measure of NAGLU substrate abundance, NAGLU enzyme activity and the efficacy of ERT in this lysosomal storage disease models studied here. The data demonstrate that CSF levels of HS-NRE is a biomarker of TA pharmacodynamic activity and suggest that sustained normalization of CSF HS-NRE could be an appropriate surrogate endpoint reasonably likely to predict clinical benefit in humans.

The HS and HS-NRE levels in CSF and CNS tissue are reduced to near normal levels within weeks of weekly dosing with TA, as shown in the 8-week PK/PD study. However, effects of TA on brain morphology, disease-associated pathology, and cognitive behavioral measures of learning and memory ability may only occur after a much longer treatment duration. While longer treatment durations might be required, effects of TA on resolution of hepatomegaly and preservation of cerebellar CSF volume were highly correlated with HS-NRE levels in the CSF suggesting the importance of reducing HS-NRE to near-normal levels to attain maximal efficacy.

The pathogenesis of the neuropathic manifestations of MPS, including MPS IIIB, is complex. There are interactions of oxidative stress (Trudel et al. 2015), disruption in autophagy and normal endosomal/lysosomal function (Monaco et al. 2020), and neuroinflammation (Archer et al. 2014). While it is known that stored HS can trigger a TLR4 response (Simonaro et al. 2010) resulting, in part, in astrocytosis and microgliosis (Wilkinson et al. 2012), it remains unclear whether such glial activation directly contributes to neurodegeneration in MPS IIIB. TA treatment decreased these disease manifestations in a dose-dependent trend as demonstrated in the IBA-1 and GFAP immunostaining presented.

The therapeutic pharmacological benefits of direct CNS administration of TA upon MPS IIIB-associated brain morphology measured by MRI were correlated in time with the improvements observed in cognitive assessments, specifically T-maze reversal learning tasks. The final T-Maze session and the final MRI sessions both occurred when the MPS IIIB dogs were approximately 2 years of age. At approximately 2 years of age, MPS IIIB dogs treated with 48 mg TA had less

cerebellar atrophy and improved cognition than MPS IIIB dogs treated with vehicle. Together with the improved neuroimmune response and lysosomal storage burden in the cerebellum and regions of the forebrain, these data suggest that less brain atrophy and disease pathology correspond to a better cognitive outcome in MPS IIIB dogs.

TA is administered directly into the CNS, bypassing any BBB exchange and restoration of NAGLU activity primarily depends on uptake by brain tissue. Therefore, one appropriate method to scale doses across species to estimate an efficacious dose for human patients is to correct for brain mass. In the present study, the 12 mg dose was selected to approximate the dose of 100 µg in mice, which previous work has shown to significantly reduce HS accumulation in brain, lysosomal dysfunctions and neuropathology when dosed twice weekly for two weeks (Aoyagi-Scharber et al. 2017). A 100 µg in mice corresponds to 250 mg in humans based on a mouse brain mass of 0.4 g. A dose of 48 mg in dogs corresponds to approximately 960 mg every other week or 480 mg weekly in humans, assuming a brain mass of 1000 g for the pediatric patient population and 50 g for dogs. The 48 mg dose in dogs was selected because it is the maximum feasible dose and it provides a sufficient safety margin over the clinical dose (300 mg weekly).

In the clinic, TA is currently administered at 300 mg weekly by ICV infusion. This dose normalizes HS and HS-NRE in the CSF within 6 weeks of treatment initiation (Muschol et al. 2021). The strong correlation between HS and HS-NRE levels in the CSF and CNS tissue in MPS IIIB dogs suggests that the CSF can be used as a surrogate compartment for predicting HS and HS-NRE levels in the CNS tissue. Normalization of HS in the CSF is reasonably likely to predict clinical efficacy in MPS IIIB subjects; 300 mg of TA administered in MPS IIIB subjects should normalize HS in CNS tissue and preserve brain volumes and functions. Indeed, reversal of hepatomegaly and cortical gray matter atrophy associated with MPS IIIB are observed in patients treated with TA and these effects are maintained out to more than 2 years (Muschol et al. 2001).

Taken together, the data presented here support the current human clinical dose of TA for the treatment of MPS IIIB disease and suggest that ICV administration can affect disease manifestations in both CNS and peripheral compartments.

JPET Fast Forward. Published on June 18, 2022 as DOI: 10.1124/jpet.122.001119
This article has not been copyedited and formatted. The final version may differ from this version.

Acknowledgements

Authors thank the animal care and veterinary staff of the ISU Laboratory Animals Resources, and the many ISU undergraduates for their assistance with animal care and production, as well as Amy Leurinda (nee Wakumoto), Carol Lien (nee Nguyen), Khoi Mai, and Cory Caprio for their help with the MRI-related endpoints. Additionally, authors thank the many people at BioMarin Pharmaceutical Inc., Northern Biomedical Research Inc., ICON Laboratory Services, Inc., KCAS and ARUP Laboratories who assisted with the studies, especially Derek Kennedy, Randall P. Reed, Eric Adams, Robert B. Boyd, Jami L. Trombley, and Dan Wendt.

Authorship Contributions

Research Design: Ellinwood, Millman, Butt, Cooper, Nestrasil, Mueller, Vuillemenot, O'Neill, Pinkstaff, Wait, Grover, Cherukuri, and Chandra

Project administration and supervision: Ellinwood, Millman, Cooper, Nestrasil, Vuillemenot, Wait, O'Neill, Pinkstaff, and McCullagh

Conducted experiments: Ellinwood, Valentine, Hess, Jens, Snella, Jamil, Hostetter, Jeffery, Smith, Parsons, Millman, Butt, Egeland, Assis, Nelvagal, Nestrasil, Prill, Liu, Zhou, Lawrence

Performed data analysis: Ellinwood, Valentine, Hess, Millman, Parsons, Butt, Chandra, Egeland, Assis, Nelvagal, Cooper, Nestrasil, Mueller, Labounek, Paulson, Prill, Lawrence, Crawford, Grover, Cherala, Melton, Cherukuri, Pinkstaff, McCullagh, Kovalchin, Zanelli

Wrote or contributed to the writing of the manuscript: McCullagh, Ellinwood, Kovalchin, Zanelli

REFERENCE LIST

Aoyagi-Scharber, M., D. Crippen-Harmon, R. Lawrence, J. Vincelette, G. Yogalingam, H. Prill, B. K. Yip, B. Baridon, C. Vitelli, A. Lee, O. Gorostiza, E. G. Adintori, W. C. Minto, J. L. Van Vleet, B. Yates, S. Rigney, T. M. Christianson, P. M. N. Tiger, M. J. Lo, J. Holtzinger, P. A. Fitzpatrick, J. H. LeBowitz, S. Bullens, B. E. Crawford, and S. Bunting. 2017. 'Clearance of Heparan Sulfate and Attenuation of CNS Pathology by Intracerebroventricular BMN 250 in Sanfilippo Type B Mice', *Mol Ther Methods Clin Dev*, 6: 43-53.

Archer, L. D., K. J. Langford-Smith, B. W. Bigger, and J. E. Fildes. 2014. 'Mucopolysaccharide diseases: a complex interplay between neuroinflammation, microglial activation and adaptive immunity', *J Inherit Metab Dis*, 37: 1-12.

Dierenfeld, A. D., M. F. McEntee, C. A. Vogler, C. H. Vite, A. H. Chen, M. Passage, S. Le, S. Shah, J. K. Jens, E. M. Snella, K. L. Kline, J. D. Parkes, W. A. Ware, L. E. Moran, A. J. Fales-Williams, J. A. Wengert, R. D. Whitley, D. M. Betts, A. M. Boal, E. A. Riedesel, W. Gross, N. M. Ellinwood, and P. I. Dickson. 2010. 'Replacing the Enzyme alpha-L-Iduronidase at Birth Ameliorates Symptoms in the Brain and Periphery of Dogs with Mucopolysaccharidosis Type I', *Science Translational Medicine*, 2: 8.

Egeland, M. T., M. M. Tarczyluk-Wells, M. M. Asmar, E. G. Adintori, R. Lawrence, E. M. Snella, J. K. Jens, B. E. Crawford, J. C. M. Wait, E. McCullagh, J. Pinkstaff, J. D. Cooper, and N. M. Ellinwood. 2020. 'Central nervous system pathology in preclinical MPS IIIB dogs reveals progressive changes in clinically relevant brain regions', *Sci Rep*, 10: 20365.

Ellinwood, N. M., P. Wang, T. Skeen, N. J. H. Sharp, M. Cesta, S. Decker, N. J. Edwards, I. Bublot, J. N. Thompson, W. Bush, E. Hardam, M. E. Haskins, and U. Giger. 2003. 'A model of mucopolysaccharidosis IIIB (Sanfilippo syndrome type IIIB): N-acetyl-alpha-D-glucosaminidase deficiency in Schipperke dogs', *Journal of Inherited Metabolic Disease*, 26: 489-504.

Ellinwood, N. Matthew, Jérôme Ausseil, Nathalie Desmaris, Stéphanie Bigou, Song Liu, Jackie K. Jens, Elizabeth M. Snella, Eman E. A. Mohammed, Christopher B. Thomson, Sylvie Raoul, Béatrice Joussemet, Françoise Roux, Yan Chérel, Yaouen Lajat, Monique Piraud, Rachid Benchaouir, Stephan Hermening, Harald Petry, Roseline Froissart, Marc Tardieu, Carine Ciron, Philippe Moullier, Jennifer Parkes, Karen L. Kline, Irène Maire, Marie-Thérèse Vanier, Jean-Michel Heard, and Marie-Anne Colle. 2011. 'Safe, efficient, and reproducible gene therapy of the brain in the dog models of Sanfilippo and Hurler syndromes', *Molecular therapy : the journal of the American Society of Gene Therapy*, 19: 251-59.

Grover, A., D. Crippen-Harmon, L. Nave, J. Vincelette, J. C. M. Wait, A. C. Melton, R. Lawrence, J. R. Brown, K. A. Webster, B. K. Yip, B. Baridon, C. Vitelli, S. Rigney, T. M. Christianson, P. M. N. Tiger, M. J. Lo, J. Holtzinger, A. J. Shaywitz, B. E. Crawford, P. A. Fitzpatrick, J. H. LeBowitz, S. Bullens, M. Aoyagi-Scharber, S. Bunting, C. A. O'Neill, J. Pinkstaff, and A. Bagri. 2020. 'Translational studies of intravenous and intracerebroventricular routes of administration for CNS cellular

biodistribution for BMN 250, an enzyme replacement therapy for the treatment of Sanfilippo type B', *Drug Deliv Transl Res*, 10: 425-39.

Harm, Tyler A., Shannon J. Hostetter, Ariel S. Nenninger, Bethann N. Valentine, N. Matthew Ellinwood, and Jodi D. Smith. 2021. 'Temporospatial Development of Neuropathologic Findings in a Canine Model of Mucopolysaccharidosis IIIB', *Veterinary pathology*, 58: 205-22.

Haskins, M, M Casal, NM Ellinwood, J Melniczek, H Mazrier, and U Giger. 2002. 'Animal models for mucopolysaccharidoses and their clinical relevance', *Acta Paediatrica*, 91: 88-97.

Jenkinson, M., C. F. Beckmann, T. E. Behrens, M. W. Woolrich, and S. M. Smith. 2012. 'FSL', *Neuroimage*, 62: 782-90.

Jones, M. Z., J. Alroy, J. C. Rutledge, J. W. Taylor, E. C. Alvord, Jr., J. Toone, D. Applegarth, J. J. Hopwood, E. Skutelsky, C. Ianelli, D. Thorley-Lawson, C. Mitchell-Herpolsheimer, A. Arias, P. Sharp, W. Evans, D. Sillence, and K. T. Cavanagh. 1997. 'Human mucopolysaccharidosis IIID: clinical, biochemical, morphological and immunohistochemical characteristics', *J Neuropathol Exp Neurol*, 56: 1158-67.

Kan, S. H., M. Aoyagi-Scharber, S. Q. Le, J. Vincelette, K. Ohmi, S. Bullens, D. J. Wendt, T. M. Christianson, P. M. Tiger, J. R. Brown, R. Lawrence, B. K. Yip, J. Holtzinger, A. Bagri, D. Crippen-Harmon, K. N. Vondrak, Z. Chen, C. M. Hague, J. C. Woloszynek, D. S. Cheung, K. A. Webster, E. G. Adintori, M. J. Lo, W. Wong, P. A. Fitzpatrick, J. H. LeBowitz, B. E. Crawford, S. Bunting, P. I. Dickson, and E. F. Neufeld. 2014. 'Delivery of an enzyme-IGFII fusion protein to the mouse brain is therapeutic for mucopolysaccharidosis type IIIB', *Proc Natl Acad Sci U S A*, 111: 14870-5.

Kan, S. H., L. A. Troitskaya, C. S. Sinow, K. Haitz, A. K. Todd, A. Di Stefano, S. Q. Le, P. I. Dickson, and B. L. Tippin. 2014. 'Insulin-like growth factor II peptide fusion enables uptake and lysosomal delivery of alpha-N-acetylglucosaminidase to mucopolysaccharidosis type IIIB fibroblasts', *Biochem J*, 458: 281-9.

Kong, W., S. Wu, J. Zhang, C. Lu, Y. Ding, and Y. Meng. 2021. 'Global epidemiology of mucopolysaccharidosis type III (Sanfilippo syndrome): an updated systematic review and meta-analysis', *J Pediatr Endocrinol Metab*, 34: 1225-35.

Laughlin, K., and M. Mendl. 2000. 'Pigs shift too: foraging strategies and spatial memory in the domestic pig', *Anim Behav*, 60: 403-10.

Lawrence, R., J. R. Brown, K. Al-Mafraji, W. C. Lamanna, J. R. Beitel, G. J. Boons, J. D. Esko, and B. E. Crawford. 2012. 'Disease-specific non-reducing end carbohydrate biomarkers for mucopolysaccharidoses', *Nat Chem Biol*, 8: 197-204.

Lawrence, R., J. R. Brown, F. Lorey, P. I. Dickson, B. E. Crawford, and J. D. Esko. 2014. 'Glycan-based biomarkers for mucopolysaccharidoses', *Mol Genet Metab*, 111: 73-83.

Li, H. H., W. H. Yu, N. Rozengurt, H. Z. Zhao, K. M. Lyons, S. Anagnostaras, M. S. Fanselow, K. Suzuki, M. T. Vanier, and E. F. Neufeld. 1999. 'Mouse model of Sanfilippo syndrome type B produced by targeted disruption of the gene encoding alpha-N-acetylglucosaminidase', *Proceedings of the National Academy of Sciences of the United States of America*, 96: 14505-10.

Monaco, A., V. Maffia, N. C. Sorrentino, I. Sambri, Y. Ezhova, T. Giuliano, V. Cacace, E. Nusco, M. De Risi, E. De Leonibus, T. Schrader, F. G. Klärner, G. Bitan, and A. Fraldi. 2020. 'The Amyloid Inhibitor CLR01 Relieves Autophagy and Ameliorates

Neuropathology in a Severe Lysosomal Storage Disease', *Molecular therapy : the journal of the American Society of Gene Therapy*, 28: 1167-76.

Muschol, N., K. von Cossel, I. Okur, F. Ezgu, M. D. Lopez, M. L. Couce, P. Harmatz, S. Batzios, M. Cleary, M. Solano, S. P. Lin, R. Giugliani, H. Amartino, H. Peters, J. Lee, J. Kovalchin, E. Zanelli, and S. Maricich. 2021. 'Tralesinidase alfa (AX 250) enzyme replacement therapy for Sanfilippo syndrome type B', *Molecular Genetics and Metabolism*, 132: S75-S75.

Neufeld, Elizabeth F., and Joseph Muenzer. 2019. 'The Mucopolysaccharidoses.' in David L. Valle, Stylianos Antonarakis, Andrea Ballabio, Arthur L. Beaudet and Grant A. Mitchell (eds.), *The Online Metabolic and Molecular Bases of Inherited Disease* (McGraw-Hill Education: New York, NY).

Nidiffer, F. D., and T. E. Kelly. 1983. 'Devevelopmental and degenerative patterns associated with cognitive, behavioral and motor difficulites in the Sanfilippo syndrome- An epidemiological- study ', *Journal of Mental Deficiency Research*, 27: 185-203.

Raj, K., N. M. Ellinwood, and U. Giger. 2020. 'An exonic insertion in the NAGLU gene causing Mucopolysaccharidosis IIIB in Schipperke dogs', *Sci Rep*, 10: 3170.

Sanders, D. N., S. Kanazono, F. A. Wininger, R. E. Whiting, C. A. Flournoy, J. R. Coates, L. J. Castaner, D. P. O'Brien, and M. L. Katz. 2011. 'A reversal learning task detects cognitive deficits in a Dachshund model of late-infantile neuronal ceroid lipofuscinosis', *Genes Brain Behav*, 10: 798-804.

Shapiro, E., K. King, A. Ahmed, K. Rudser, R. Rumsey, B. Yund, K. Delaney, I. Nestrasil, C. Whitley, and M. Potegal. 2016. 'The Neurobehavioral Phenotype in Mucopolysaccharidosis Type IIIB: an Exploratory Study', *Molecular genetics and metabolism reports*, 6: 41-47.

Simonaro, C. M., Y. Ge, E. Eliyahu, X. He, K. J. Jepsen, and E. H. Schuchman. 2010. 'Involvement of the Toll-like receptor 4 pathway and use of TNF-alpha antagonists for treatment of the mucopolysaccharidoses', *Proc Natl Acad Sci U S A*, 107: 222-7.

Singer, M. . 1962. *The Brain of the Dog in Section* (Saunders: Philadelphia, PA).

Troy, S., M. Wasilewski, J. Beusmans, and C. J. Godfrey. 2020. 'Pharmacokinetic Modeling of Intrathecally Administered Recombinant Human Arylsulfatase A (TAK-611) in Children With Metachromatic Leukodystrophy', *Clin Pharmacol Ther*, 107: 1394-404.

Trudel, S., E. Trécherel, C. Gomila, M. Peltier, M. Aubignat, B. Gubler, P. Morlière, J. M. Heard, and J. Ausseil. 2015. 'Oxidative stress is independent of inflammation in the neurodegenerative Sanfilippo syndrome type B', *J Neurosci Res*, 93: 424-32.

Valstar, M. J., J. P. Marchal, M. Grootenhuis, V. Colland, and F. A. Wijburg. 2011. 'Cognitive development in patients with Mucopolysaccharidosis type III (Sanfilippo syndrome)', *Orphanet Journal of Rare Diseases*, 6: 6.

Valstar, M. J., G. J. Ruijter, O. P. van Diggelen, B. J. Poorthuis, and F. A. Wijburg. 2008. 'Sanfilippo syndrome: a mini-review', *J Inherit Metab Dis*, 31: 240-52.

Vuillemenot, B. R., D. Kennedy, R. P. Reed, R. B. Boyd, M. T. Butt, D. G. Musson, S. Keve, R. Cahayag, L. S. Tsuruda, and C. A. O'Neill. 2014. 'Recombinant human tripeptidyl peptidase-1 infusion to the monkey CNS: safety, pharmacokinetics, and distribution', *Toxicol Appl Pharmacol*, 277: 49-57.

Wang, B., B. Yu, M. Karim, H. H. Hu, Y. Sun, P. McGreevy, P. Petocz, S. Held, and J. Brand-Miller. 2007. 'Dietary sialic acid supplementation improves learning and memory in piglets', *American Journal of Clinical Nutrition*, 85: 561-69.

Weber, B., J. J. Hopwood, and G. Yogalingam. 2001. 'Expression and characterization of human recombinant and alpha-N-acetylglucosaminidase', *Protein Expr Purif*, 21: 251-9.

Wilkinson, F. L., R. J. Holley, K. J. Langford-Smith, S. Badrinath, A. Liao, A. Langford-Smith, J. D. Cooper, S. A. Jones, J. E. Wraith, R. F. Wynn, C. L. Merry, and B. W. Bigger. 2012. 'Neuropathology in mouse models of mucopolysaccharidosis type I, IIIA and IIIB', *PLoS One*, 7: e35787.

Yogalingam, G., A. R. Luu, H. Prill, M. J. Lo, B. Yip, J. Holtzinger, T. Christianson, M. Aoyagi-Scharber, R. Lawrence, B. E. Crawford, and J. H. LeBowitz. 2019. 'BMN 250, a fusion of lysosomal alpha-N-acetylglucosaminidase with IGF2, exhibits different patterns of cellular uptake into critical cell types of Sanfilippo syndrome B disease pathogenesis', *PLoS One*, 14: e0207836.

Zafeiriou, D. I., P. A. Savvopoulou-Augoustidou, A. Sewell, F. Papadopoulou, M. Badouraki, E. Vargiami, N. P. Gombakis, and G. S. Katzos. 2001. 'Serial magnetic resonance imaging findings in mucopolysaccharidosis IIIB (Sanfilippo's syndrome B)', *Brain & Development*, 23: 385-89.

Zhang, Y., M. Brady, and S. Smith. 2001. 'Segmentation of brain MR images through a hidden Markov random field model and the expectation-maximization algorithm', *IEEE Trans Med Imaging*, 20: 45-57.

Zhao, K. W., and E. F. Neufeld. 2000. 'Purification and characterization of recombinant human alpha-N-acetylglucosaminidase secreted by Chinese hamster ovary cells', *Protein Expr Purif*, 19: 202-11.

Footnotes

Funding: This work was funded by BioMarin Pharmaceutical Inc. and Allievex Corporation. ISU authors acknowledge support from the ISU College of Agriculture and Life Sciences, the ISU College of Veterinary Medicine, the Hatch Act, and the State of Iowa. The MPS IIIB dog colony was founded at the University of Pennsylvania and was supported by the National Institutes of Health Referral Center – Animal Models of Human Genetic Disease [Grant P40OD010939]. The University of Minnesota Foundation funded the purchase of anesthesia and monitoring machines for MRI analyses.

Competing interests: HP, XL, HZ, RL, BC, AG, GC, ACM, AC, JCMW, CAO, JP, EZ, EM are, or were at the time these studies were conducted, employees and shareholders of BioMarin Pharmaceutical Inc. NME, IN, and JC have received research support from BioMarin Pharmaceutical Inc. JK and EZ are employees of Allievex Corporation. EM is a paid consultant for Allievex Corporation. All other authors have no competing interests to declare.

JPET Fast Forward. Published on June 18, 2022 as DOI: 10.1124/jpet.122.001119
This article has not been copyedited and formatted. The final version may differ from this version.

Legends for Figures

Figure 1. Pharmacodynamic effect of TA on HS and HS-NRE levels in CSF and CNS tissue of MPS IIIB dogs from the long-term efficacy study. Total HS (HS) (A, C) and the MPS IIIB-specific HS-NRE (B, D) levels were measured in CSF or CNS tissue (pooled brain and spinal cord tissue from 8-12 CNS regions/dog). (All) Number of dogs analyzed per condition is included in each of the panels. CNS tissue and CSF samples were collected within 72 hours after the last dose. Median (solid lines), 25-75%iles (boxes), individual values and data range (bars) are shown. UA dogs are shown in open circles, MPS IIIB dogs treated with vehicle are shown in closed circles, MPS IIIB dogs treated with 12 mg TA are shown in gray triangles, and MPS IIIB dogs treated with 48 mg TA are shown in open squares. Dashed line in CSF graphs represents the lower limit of quantitation (LLOQ) of the assay (0.035 µg/ml and 0.01 µg/ml for HS and HS-NRE, respectively). No LLOQ was defined for the tissue-based assay. CSF samples for which values were below the limit of quantitation were set as LLOQ/2 (0.0175 µg/ml and 0.005 µg/ml for HS and HS-NRE, respectively). *P* values were calculated using 2-sided unpaired t-tests. UA = unaffected control dogs, TA = tralesinidase alfa.

Figure 2: Correlation Analysis of HS and HS-NRE Levels in CNS Tissue and CSF in MPS IIIB Dogs Treated with Various Doses of TA. (A) HS from CNS tissue and CSF of MPS IIIB dogs from studies in Table 1 and Supplementary Table 1 were plotted and correlation by simple linear regression was assessed. Data from the long-term efficacy and 8-week PK/PD studies were included for statistical power. Sum of two internal disaccharides were used to quantify HS in CNS tissue and compare to HS levels in CSF, where the same two internal disaccharides were measured. (B) HS-NRE from CNS tissue and CSF of MPS IIIB dogs in Table 1 were plotted and correlation by simple linear regression was assessed. Correlation analysis of HS-NRE levels in dogs from Supplementary Table 1 was not possible because HS-NRE levels were BLQ. CNS tissue and CSF samples were collected within 72 hours after the last dose for dogs in Table 1 or at 1 week, 2 weeks or 4 weeks after the last dose for dogs in Supplementary Table 1.

JPET Fast Forward. Published on June 18, 2022 as DOI: 10.1124/jpet.122.001119
This article has not been copyedited and formatted. The final version may differ from this version.

Figure 3. Effects of TA treatment on LAMP1 staining in brains of MPS IIIB dog from the long-term efficacy study and correlation with CSF HS-NRE levels. A) Immunostaining in hippocampus (CA1), somatosensory cortex and cerebellar granular layer of MPS IIIB dogs using anti-LAMP1 antibody on tissues collected at necropsy. One-way ANOVA with Tukey's multiple comparison tests were conducted on data from each brain region. N = 3 (vehicle, hippocampus), N = 4 for all other regions and treatments. B) Simple linear regression was used to determine the correlation of LAMP1 immunostaining of somatosensory cortex (dashed line, triangles) and cerebellar granular layer (solid line, circles) with HS-NRE concentrations in CSF samples collected at necropsy from dogs in Table 1. The CSF HS-NRE values for normal unaffected animals is shown by the dotted line, which is also the LLOQ of the assay. N = 4 (vehicle, 48 mg TA) and n = 3 (12 mg TA). (C) Immunostaining of IBA-1 in the cerebellar white matter of MPS IIB dogs treated with vehicle (n = 4, open circles), 12 mg TA (n = 4, open triangles), or 48 mg TA (n = 4, open squares). D) Immunostaining of GFAP in two regions of the cerebellum (Bergmann glia and Purkinje Layer) of MPS IIIB dogs treated with vehicle (n = 3, open circles), 12 mg TA (n = 4, open triangles), or 48 mg TA (n = 4, open squares). One-way ANOVA tests were conducted on data from the cerebellar regions (P = 0.03 for the Purkinje layer, ns for the Bergmann glia) with Tukey's multiple comparison test (P = 0.03 for MPS IIIB Veh vs MPS IIIB 12 mg TA). TA = tralesinidase alfa.

Figure 4. Effects of TA treatment on liver size in MPS IIIB dogs from the long-term efficacy study. (A) Weights of brain, liver and heart of MPS IIIB dogs at time of necropsy. Liver weights of MPS IIIB dogs treated with vehicle or 48 mg TA were compared using multiple unpaired t tests (P = 0.002). (B) Correlation using simple linear regression between liver weight at time of necropsy and HS-NRE concentrations in CSF of MPS IIIB dogs in Table 1 at time of necropsy. The CSF HS-NRE values for normal unaffected animals is shown by the dotted line, which is also the LLOQ of the assay. (All) Data from UA dogs are shown in diamonds (n = 4), MPS IIIB dogs treated with vehicle shown in circles (n = 4), MPS IIIB dogs treated with 12 mg are shown in triangles (n = 4 for brain and liver, n = 3 for heart), and MPS IIIB dogs treated with 48 mg are shown in squares (n = 4). TA = tralesinidase alfa; UA = unaffected littermate dogs.

JPET Fast Forward. Published on June 18, 2022 as DOI: 10.1124/jpet.122.001119
This article has not been copyedited and formatted. The final version may differ from this version.

Figure 5. Effects of TA on cerebellar CSF volume and correlation with CSF HS-NRE levels. (A) Cerebellar CSF volume of dogs from the long-term efficacy study were measured by MRI on the 6th and last session (close to necropsy) when dogs were about two years old. Cerebellar CSF volumes of MPS IIIB dogs treated with 48 mg TA were compared with cerebellar CSF volumes of MPS IIIB dogs treated with vehicle (P = 0.0127, one-way ANOVA with Dunnett's multiple comparisons test). (B) Correlation by simple linear regression between cerebellar CSF volume and HS-NRE concentrations in the CSF of dogs from the dogs in Table 1 at time of necropsy. The CSF HS-NRE values for normal unaffected animals is shown by the dotted line, which is also the LLOQ of the assay. (All) MPS IIIB dogs treated with vehicle (circles, n = 3), 12 mg (triangles, n = 2) and 48 mg (squares, n = 4). UA = unaffected dogs (diamonds, n = 2); TA = tralesinidase alfa.

Figure 6. Effects of TA on performance in a T-Maze reversal learning task in MPS IIIB dogs from the long-term efficacy study. (A) Average difference in error numbers committed by each dog in Session 5 (23.5 months of age on average) versus Session 1 (14.2 months of age on average) in the T-Maze reversal learning test. Data from unaffected dogs (UA; diamonds, n = 3), or MPS IIIB dogs treated with vehicle (circles, n = 3), 12 mg TA (triangles, n = 2) or 48 mg TA (squares, n = 4) are shown. (B) Average error numbers made by each dog after the first correct choice in Session 1 and Session 5 during the reversal learning tasks for UA animals and MPS IIIB dogs treated with vehicle (n = 5 both sessions) or TA-treated (12 and 48 mg doses combined to increase statistical power; n = 7 session 1 and n = 6 session 5). Performance of dogs at Session 5 was compared to their performance at Session 1 (P values shown on graph, Adjusted t-test). UA = unaffected littermates; TA = tralesinidase alfa.

JPET Fast Forward. Published on June 18, 2022 as DOI: 10.1124/jpet.122.001119
This article has not been copyedited and formatted. The final version may differ from this version.

Tables

Table 1: Study design of the long-term efficacy study with TA in MPS IIIB dogs

Group	Phenotype	No of Animals	Dose (mg)	Dose Frequency
1	MPS IIIB	4 (2M/2F)	0	QOW
2	MPS IIIB	4 (3M/1F)	12	QOW
3	MPS IIIB	4 (1M/3F)	48	QOW

Figure 1

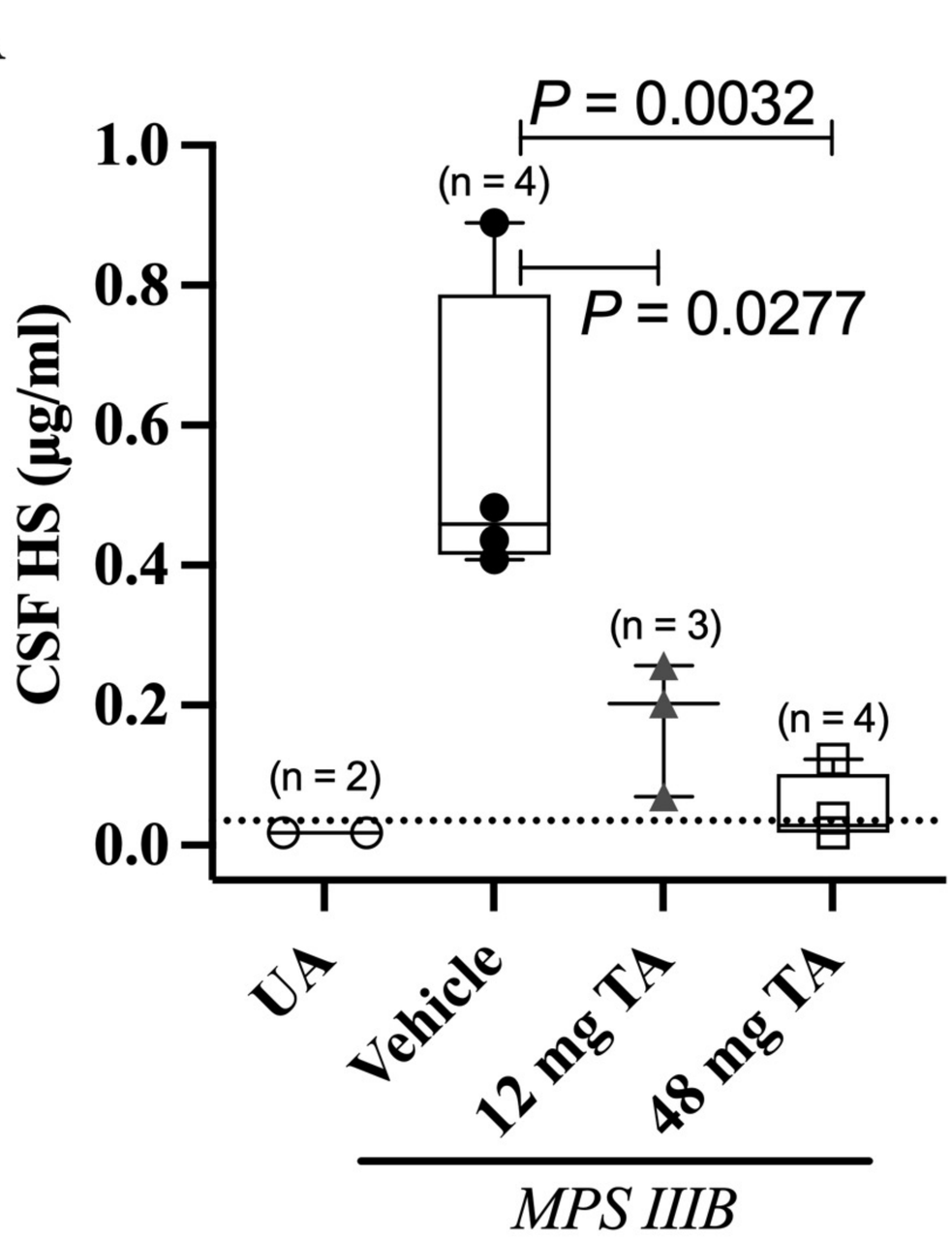

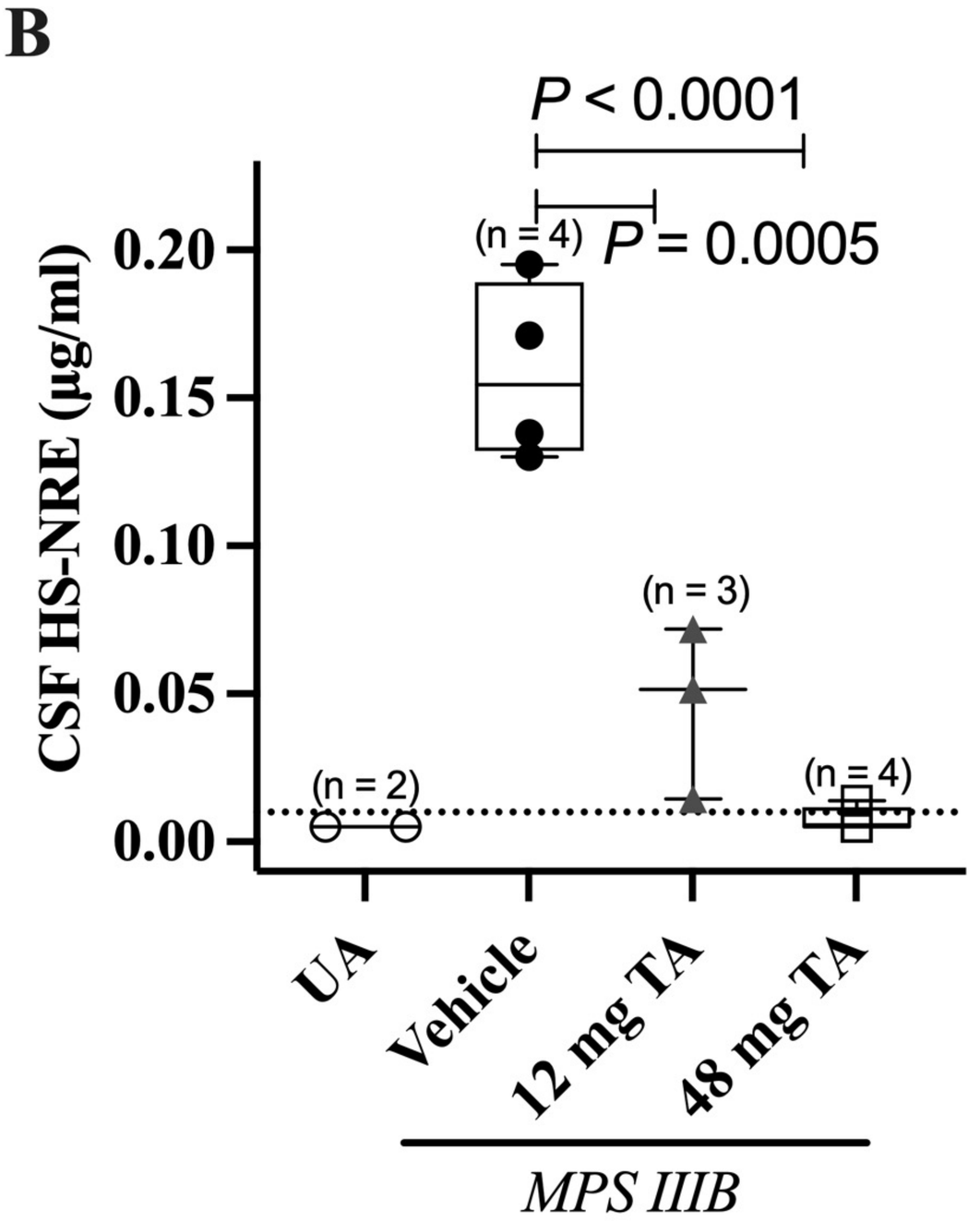

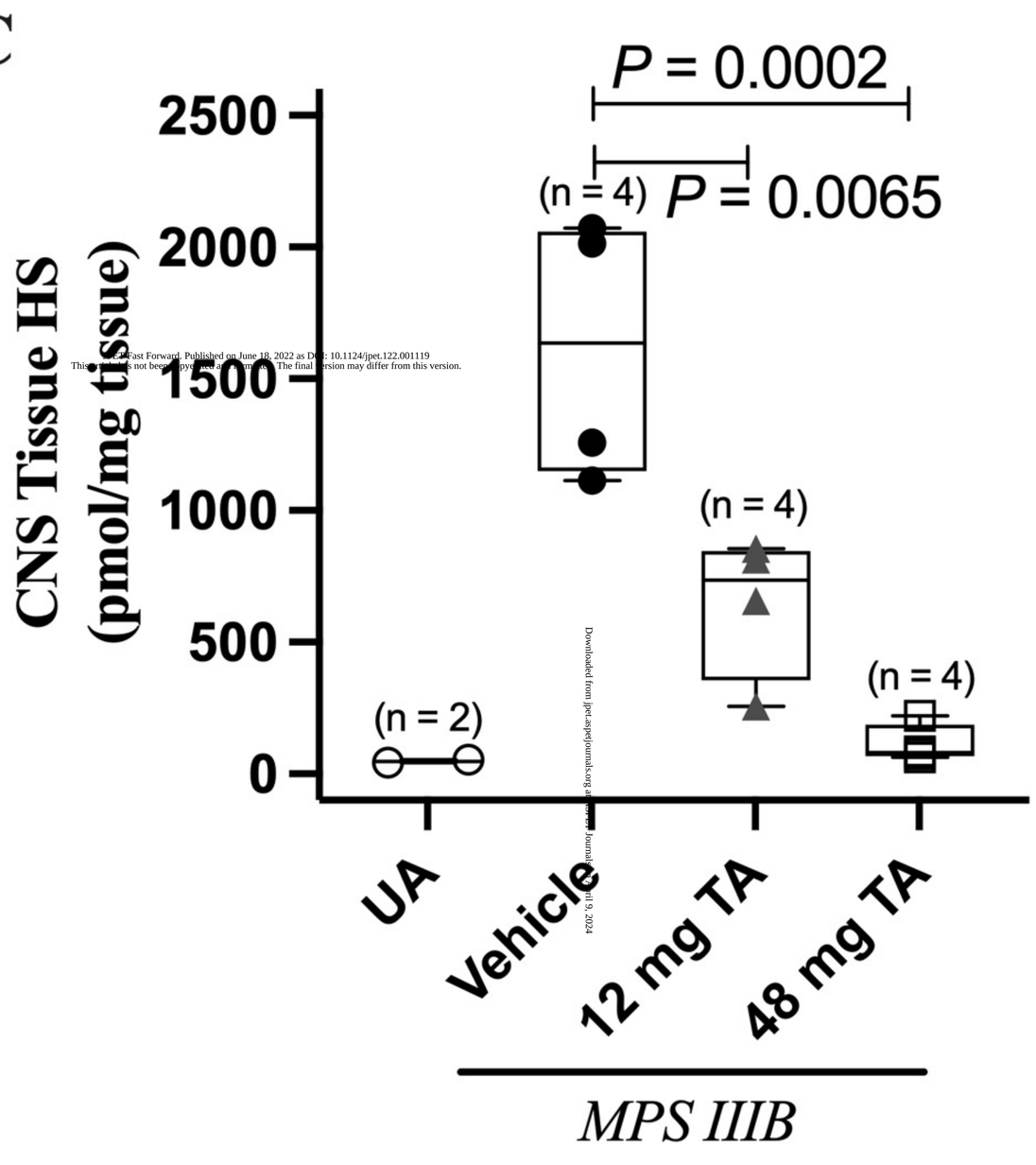

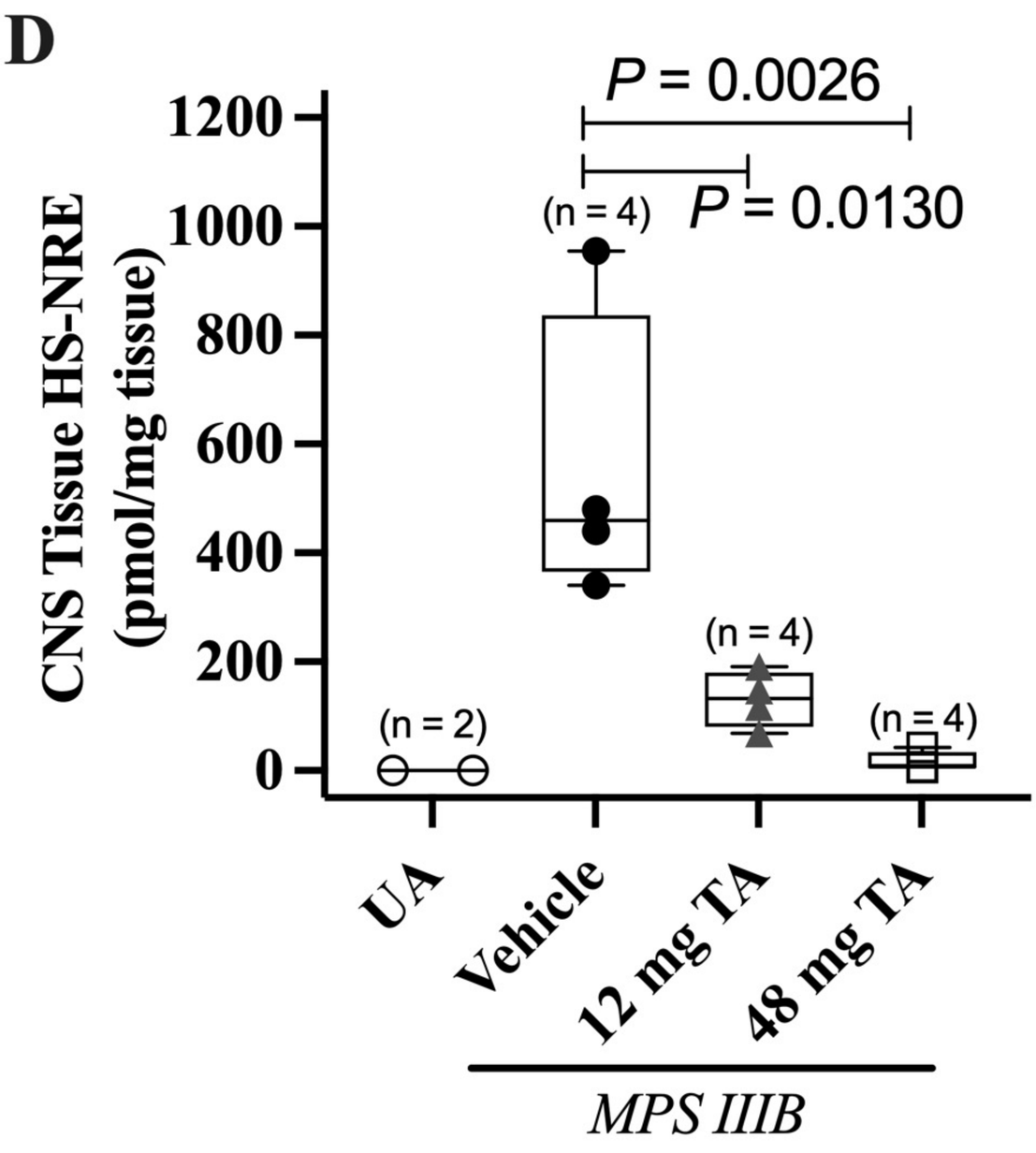

Figure 2

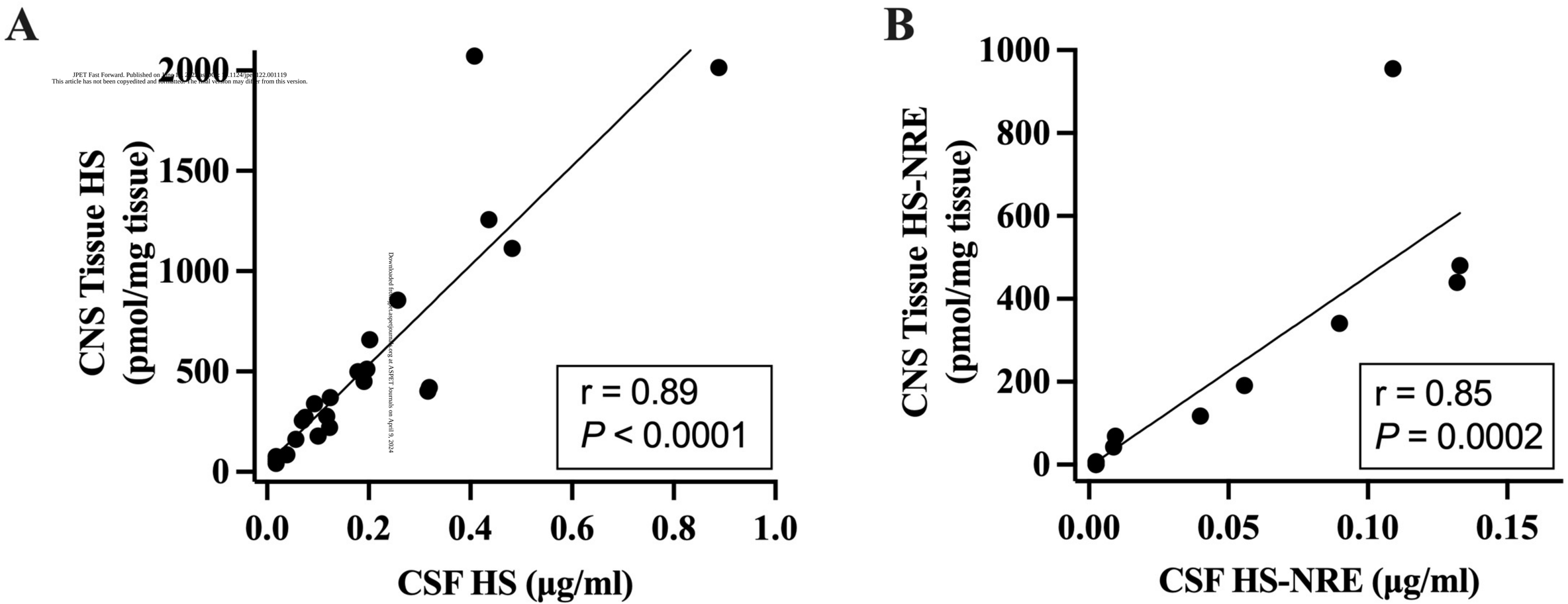

Figure 3

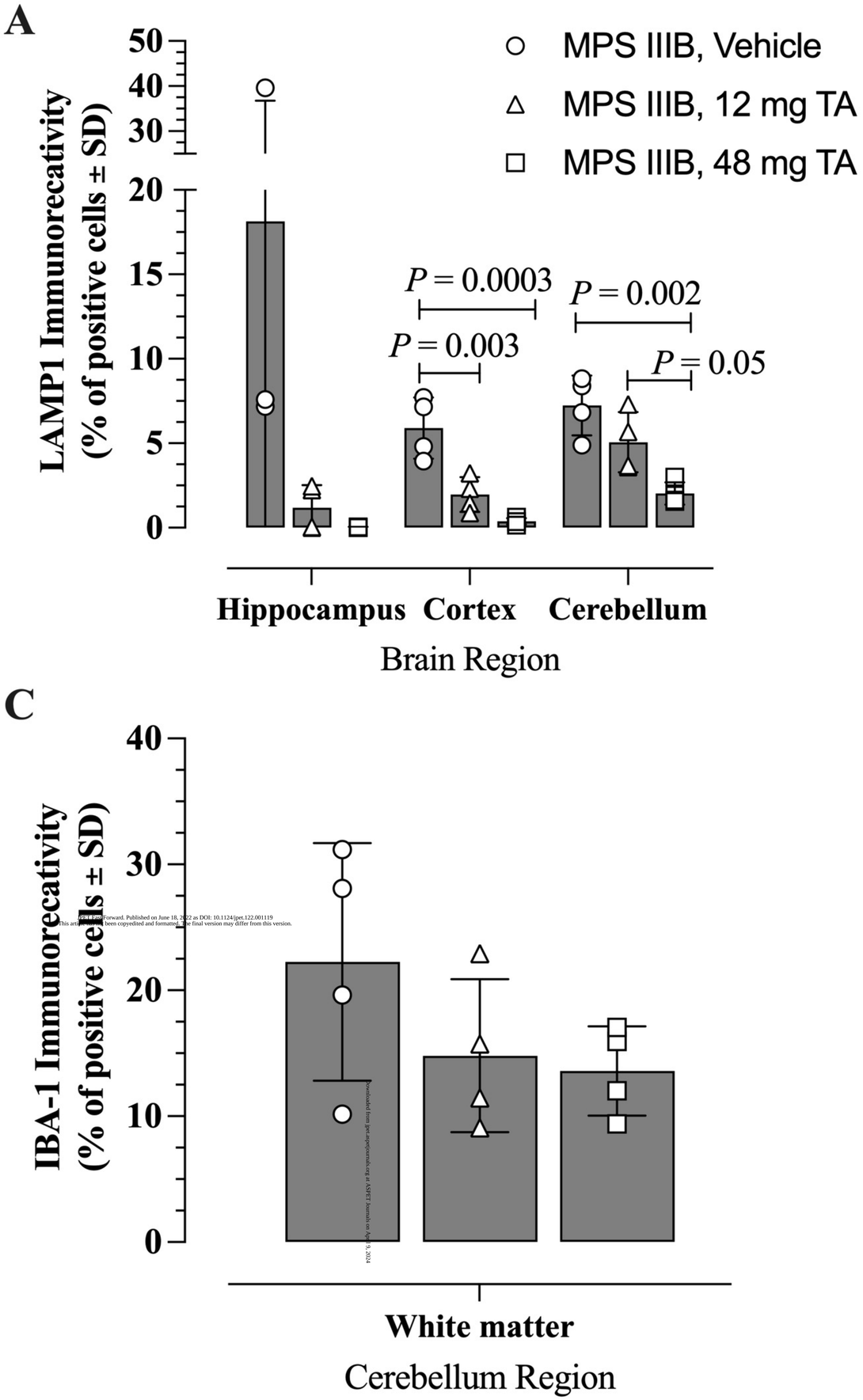

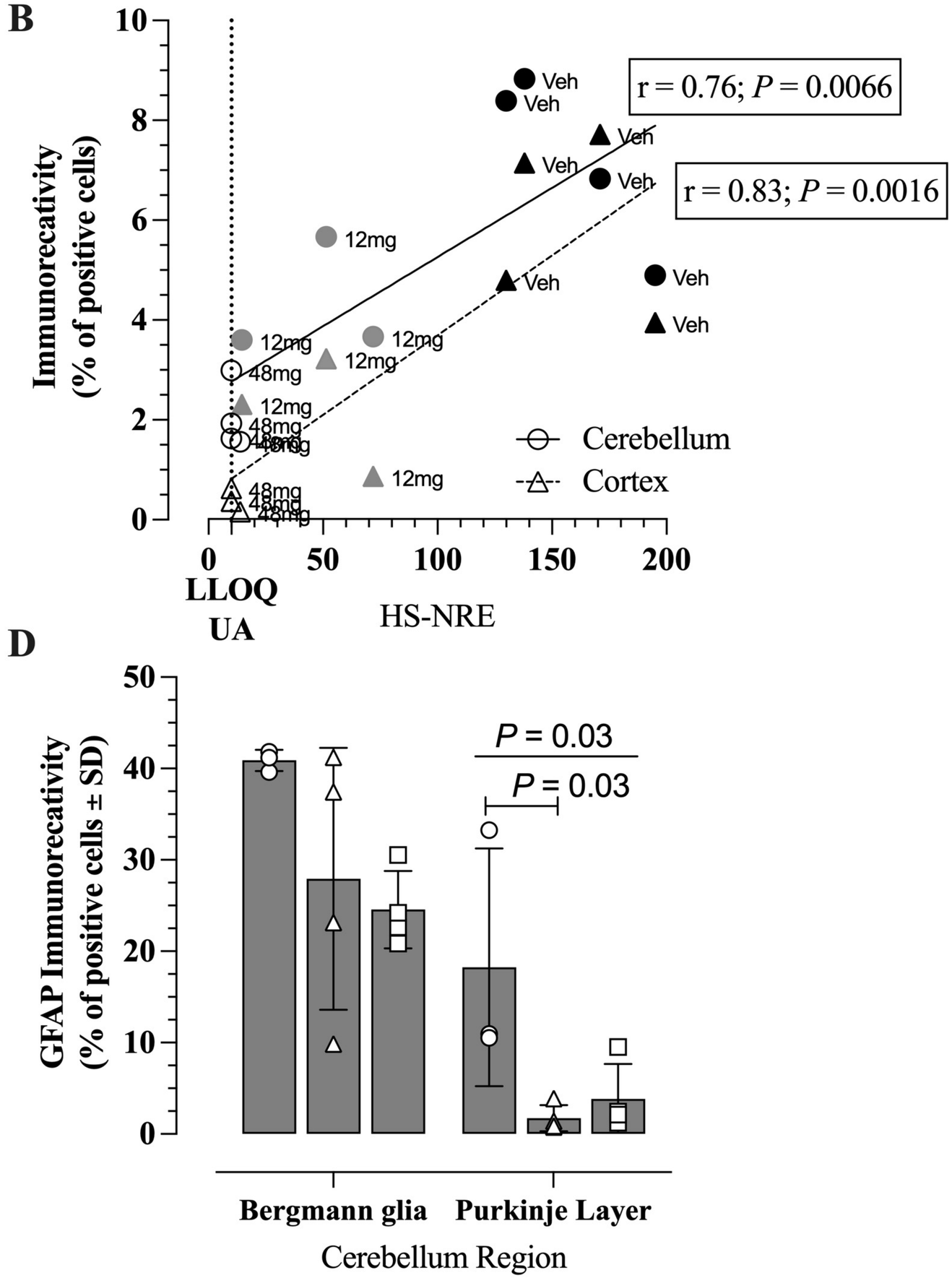

Figure 4

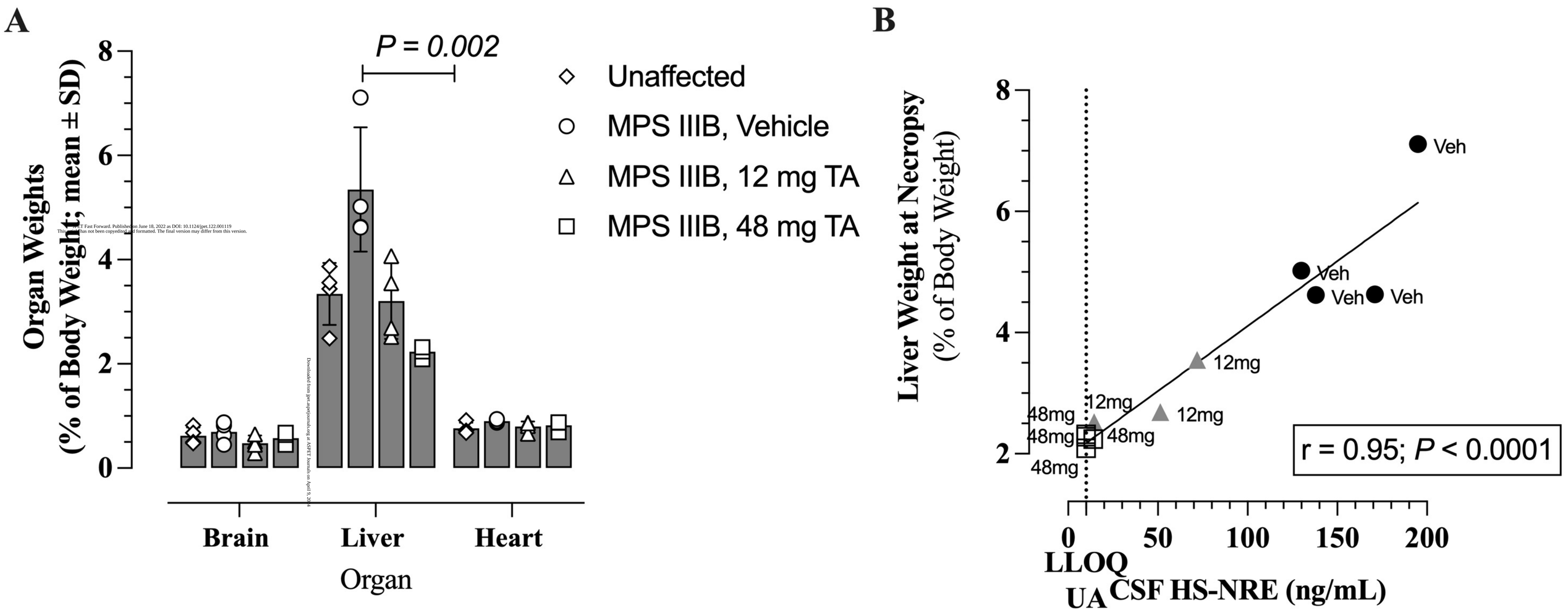

Figure 5

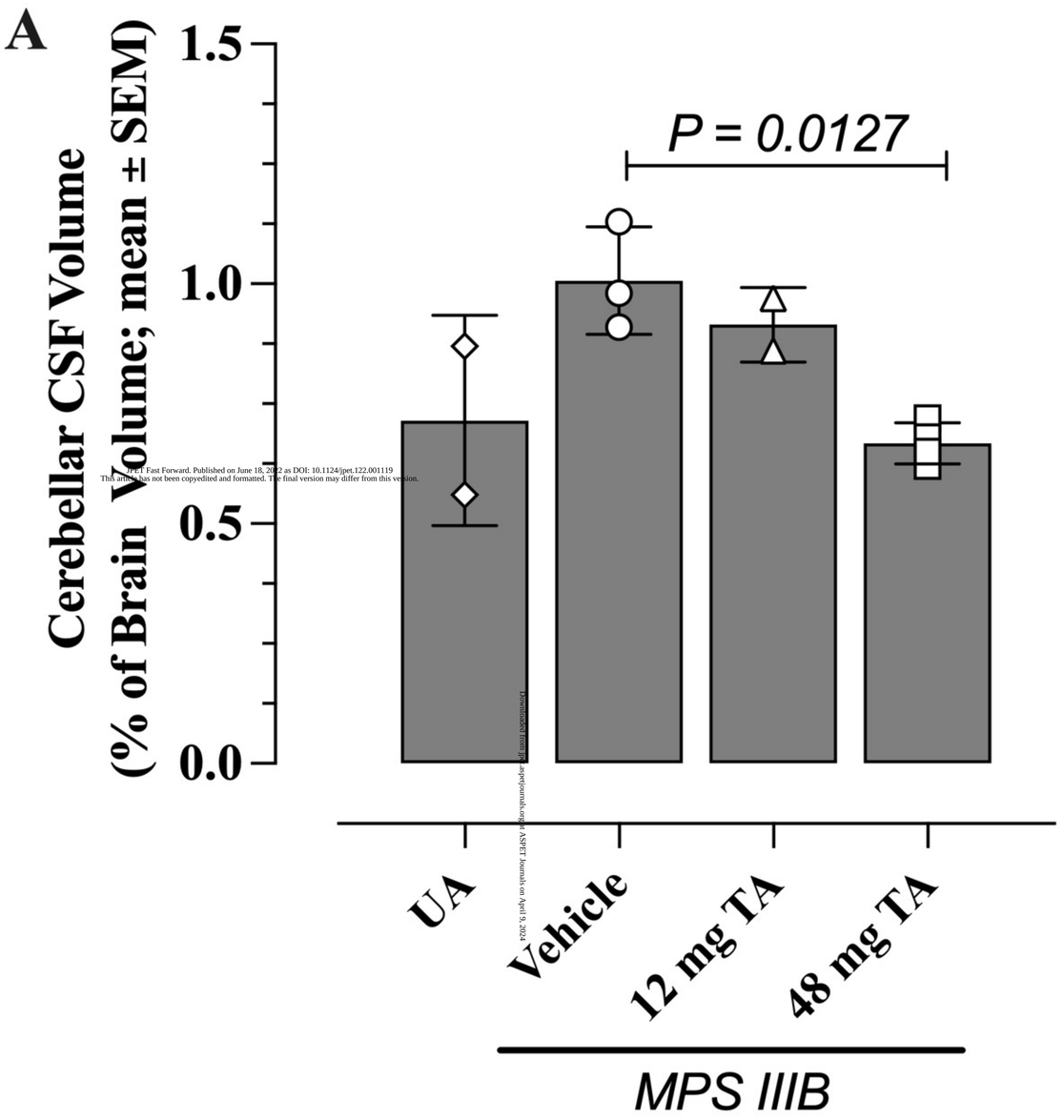

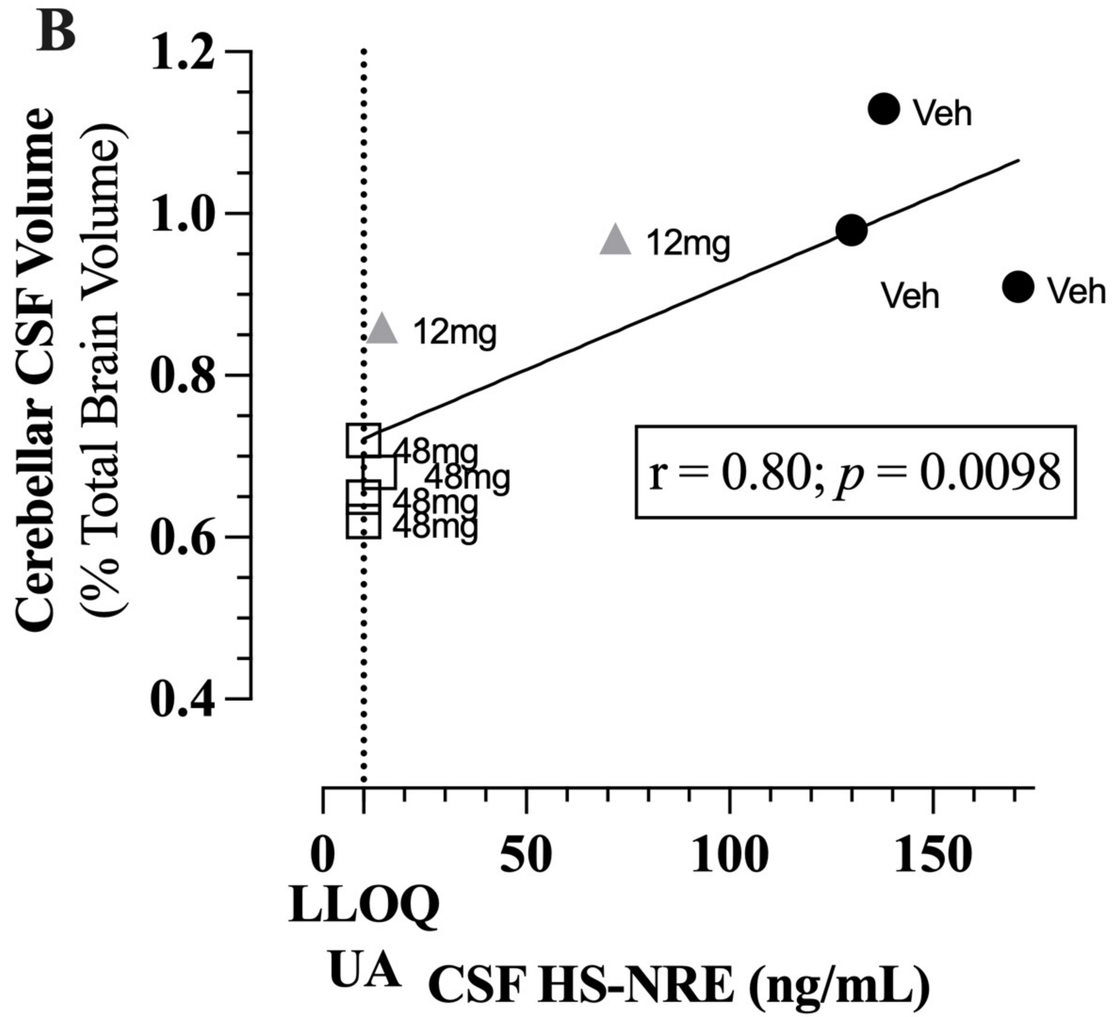

Figure 6

A

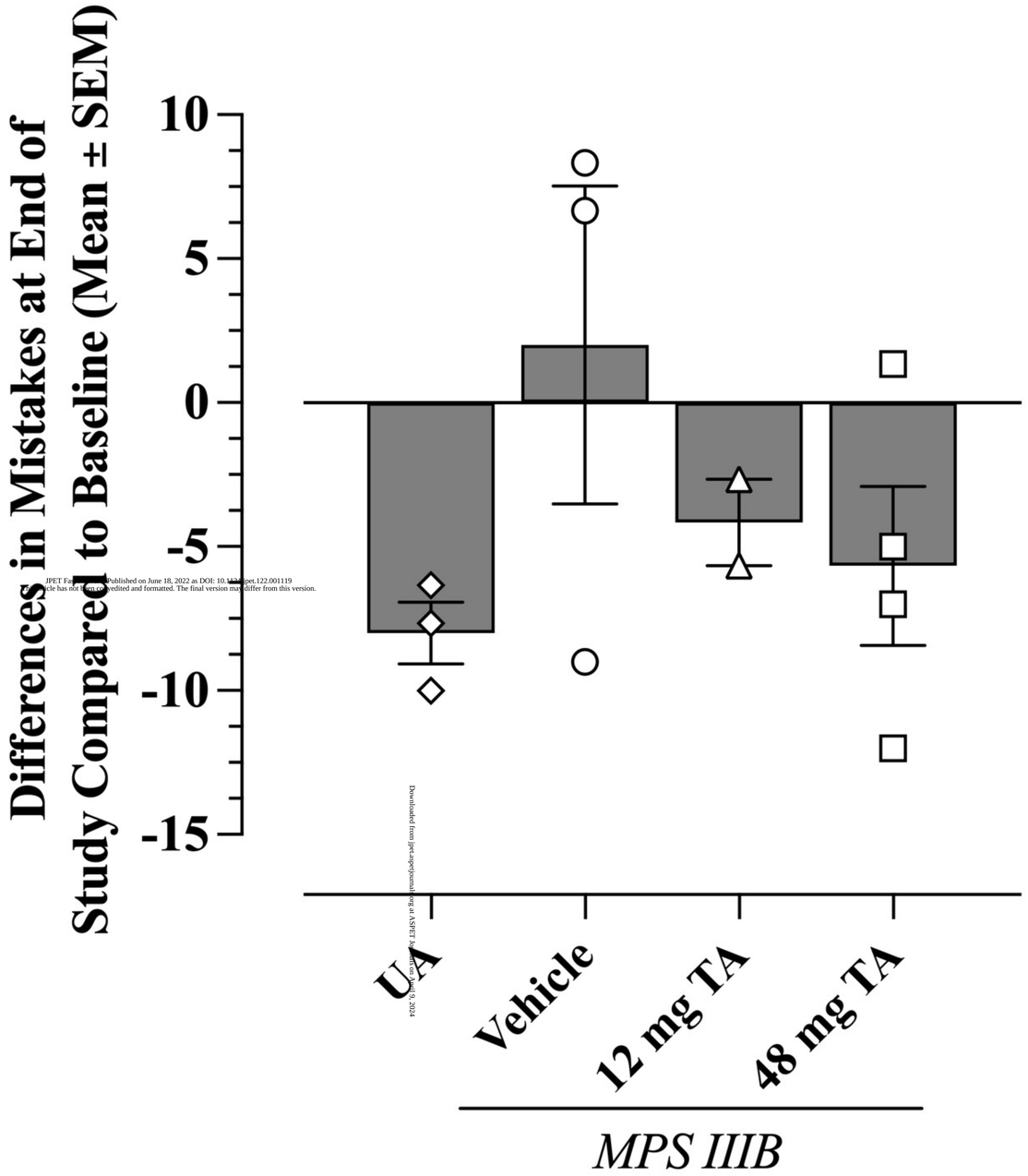

B